OPEN ACCESS Freely available online

PLoS PATHOGENS

The Microbiota Mediates Pathogen Clearance from the Gut Lumen after Non-Typhoidal *Salmonella* Diarrhea

Kathrin Endt[1☯], Bärbel Stecher[1☯], Samuel Chaffron[2], Emma Slack[3], Nicolas Tchitchek[4], Arndt Benecke[4], Laurye Van Maele[5], Jean-Claude Sirard[5], Andreas J. Mueller[1], Mathias Heikenwalder[6], Andrew J. Macpherson[3], Richard Strugnell[7], Christian von Mering[2], Wolf-Dietrich Hardt[1]*

1 Institute of Microbiology, ETH Zürich, Zürich, Switzerland, **2** Institute of Molecular Biology and Swiss Institute of Bioinformatics, University of Zürich, Zürich, Switzerland, **3** Gastroenterology Inselspital, Department Klinische Forschung, Bern, Switzerland, **4** Institut des Hautes Études Scientifiques & CNRS USR3078, Bures sur Yvette, France, **5** Institut National de la Santé et de la Recherche Médicale, U801; Institut Pasteur de Lille; Univ. Lille Nord de France, UDSL, Lille, France, **6** Institute of Neuropathology, University Hospital of Zurich, Zürich, Switzerland, **7** Department of Microbiology and Immunology, The University of Melbourne, Parkville, Victoria, Australia

Abstract

Many enteropathogenic bacteria target the mammalian gut. The mechanisms protecting the host from infection are poorly understood. We have studied the protective functions of secretory antibodies (sIgA) and the microbiota, using a mouse model for *S. typhimurium* diarrhea. This pathogen is a common cause of diarrhea in humans world-wide. *S. typhimurium* (*S. tm*^{att}, *sseD*) causes a self-limiting gut infection in streptomycin-treated mice. After 40 days, all animals had overcome the disease, developed a sIgA response, and most had cleared the pathogen from the gut lumen. sIgA limited pathogen access to the mucosal surface and protected from gut inflammation in challenge infections. This protection was O-antigen specific, as demonstrated with pathogens lacking the *S. typhimurium* O-antigen (*wbaP*, *S. enteritidis*) and sIgA-deficient mice (TCR$\beta^{-/-}\delta^{-/-}$, $J_H^{-/-}$, $IgA^{-/-}$, $pIgR^{-/-}$). Surprisingly, sIgA-deficiency did not affect the kinetics of pathogen clearance from the gut lumen. Instead, this was mediated by the microbiota. This was confirmed using 'L-mice' which harbor a low complexity gut flora, lack colonization resistance and develop a normal sIgA response, but fail to clear *S. tm*^{att} from the gut lumen. In these mice, pathogen clearance was achieved by transferring a normal complex microbiota. Thus, besides colonization resistance (= pathogen blockage by an intact microbiota), the microbiota mediates a second, novel protective function, i.e. pathogen clearance. Here, the normal microbiota re-grows from a state of depletion and disturbed composition and gradually clears even very high pathogen loads from the gut lumen, a site inaccessible to most "classical" immune effector mechanisms. In conclusion, sIgA and microbiota serve complementary protective functions. The microbiota confers colonization resistance and mediates pathogen clearance in primary infections, while sIgA protects from disease if the host re-encounters the same pathogen. This has implications for curing *S. typhimurium* diarrhea and for preventing transmission.

Citation: Endt K, Stecher B, Chaffron S, Slack E, Tchitchek N, et al. (2010) The Microbiota Mediates Pathogen Clearance from the Gut Lumen after Non-Typhoidal *Salmonella* Diarrhea. PLoS Pathog 6(9): e1001097. doi:10.1371/journal.ppat.1001097

Editor: C. Erec Stebbins, The Rockefeller University, United States of America

Received May 19, 2010; **Accepted** August 11, 2010; **Published** September 9, 2010

Copyright: © 2010 Endt et al. This is an open-access article distributed under the terms of the Creative Commons Attribution License, which permits unrestricted use, distribution, and reproduction in any medium, provided the original author and source are credited.

Funding: This work was supported by grants from the Swiss National Science Foundation (310000-113623/1, to WDH), the Promedica Foundation (1097/A to WDH), the European Union (SavinMucoPath No. 032296, to WDH and JCS), the Agence Nationale de la Recherche (ISPA, 07-PHYSIO-013-02, to AB) and the Génopole Evry (to AB). The funders had no role in study design, data collection and analysis, decision to publish, or preparation of the manuscript.

Competing Interests: The authors have declared that no competing interests exist.

* E-mail: hardt@micro.biol.ethz.ch

☯ These authors contributed equally to this work.

Introduction

Bacterial diarrhea is a global cause of morbidity and mortality. In most cases, the acute disease symptoms cease after a few days and the pathogen is eliminated from the gut. However, the mechanisms eliminating enteropathogenic bacteria from the gut lumen are poorly understood. Most "classical" effector mechanisms of the immune system are ineffective in the gut lumen (i.e. complement-mediated killing, opsonophagocytosis, T-cell mediated toxicity). In the gut, innate and adaptive immune responses such as antimicrobial peptides, natural and pathogen-specific mucosal secretory IgA (sIgA) antibodies are considered to be cardinal defense mechanisms. In addition to the host's immune system, the highly dense and diverse bacterial community in the gut (the microbiota; >500 different species [1,2]) plays a key role by inhibiting pathogen growth in the gut lumen right from the beginning. This phenomenon is referred to as 'colonization resistance' and efficiently blocks infections by *Clostridium difficile*, *Salmonella* spp. and many other pathogenic bacteria [3]. Colonization resistance might be based on nutrient limitation, release of inhibitory metabolites, production of bactericidal compounds, the competition for binding sites and other, unidentified features of the dense microbial community [4,5].

Much less is known about the mechanisms clearing enteropathogenic bacteria from the gut lumen once they have established an infection in this niche. 'Pathogen clearance' differs significantly from colonization resistance as both, the mucosa [6] and the microbiota, must recover from pathogen-inflicted disturbance while eliminating the pathogen [7]. Here, we have studied the mechanisms of pathogen clearance from the gut lumen using the example of non-typhoidal *Salmonella* (NTS) diarrhea.

NTS infections, including *S. enterica* spp. I serovar Typhimurium (*S. tm*), account for a significant share of food-borne diarrhea in

Author Summary

Numerous pathogens infect the gut. Protection against these infections is mediated by mucosal immune defenses including secreted IgA as well as by the competing intestinal microbiota. However, so far the relative importance of these two different defense mechanisms remains unclear. We addressed this question using the example of non-typhoidal *Salmonella* (NTS) gut infections which can be spread in stool of infected patients over long periods of time. We used a mouse model to reveal that the intestinal microbiota and the adaptive immune system hold different but complementary functions in fighting NTS infections. A primary *Salmonella* infection disrupts the normal microbiota and elicits *Salmonella*-specific sIgA. sIgA prevents disease when the animal is infected with NTS for a second time. However, sIgA was dispensable for pathogen clearance from the gut. Instead, this was mediated by the microbiota. By re-establishing its normal density and composition, the microbiota was necessary and sufficient for terminating long-term fecal *Salmonella* excretion. This establishes a novel paradigm: The microbiota clears the pathogen from the gut lumen, while sIgA protects from disease upon re-infection with the same pathogen. This has implications for the evolutionary role of sIgA responses as well as for developing microbiota-based therapies for curing infected patients.

Europe and Northern America. In sub-Saharan Africa, NTS are also an important cause of invasive disease with high mortality, particularly in HIV infected individuals [8]. In humans, colonization resistance confers partial protection, but antibiotic treatment increases the risk of *Salmonella* diarrhea [9,10]. In the typical cases of NTS diarrhea, the pathogen begins to grow in the gut and disease symptoms manifest eight to 24h after consumption of contaminated food or water. Usually, the pathogen remains limited to the gastrointestinal tract and diarrhea subsides within several days. After cessation of symptoms, *Salmonella* remains detectable in the stool for weeks, several months or sometimes even longer [11,12]. Pathogen clearance seems to fail in these long-term 'asymptomatic excretors'. This is problematic, as 'asymptomatic excretors' pose a significant risk of transmission, in particular when food workers in restaurants or the food industry are affected [13].

So far, we can only speculate about mechanisms mediating pathogen clearance from the gut lumen. Antimicrobial peptides might be involved in some infections, but should not affect *S. tm* clearance, as this pathogen is particularly resistant against this type of compound [14,15]. Antibody responses, i.e. pathogen-specific secretory IgA (sIgA), might also clear pathogens from the gut lumen. *S. tm* elicits profound antibody responses against LPS and protein antigens [16]. In systemic infection models antibody responses can confer some degree of protection [17,18]. Previous work on the role of sIgA in intestinal *S. tm* infection yielded conflicting results. sIgA protected cultured epithelial cells from *S. tm* infection, but did not reduce intestinal pathogen densities [18]. Similar findings were made for the enteropathogenic bacterium *Citrobacter rodentium* [19]. However, the role of sIgA in pathogen clearance in models of acute *Salmonella* enterocolitis with high intestinal pathogen loads has not been addressed so far. Finally, we reasoned that the microbiota itself might contribute to pathogen clearance. It remained to be shown which mechanisms contribute to pathogen clearance.

We have used a *Salmonella* diarrhea mouse model to analyze the relative importance of sIgA and the intestinal microbiota in *S. tm* clearance after infection. In mice, the intestinal microbiota confers colonization resistance. Normally, $<10\%$ of mice permit pathogen growth and get mucosal inflammation upon oral *S. tm* infection [20]. Oral antibiotic-treatment alleviates colonization resistance and wild type *S. tm* grows up to very high densities in the intestinal lumen and induces mucosal inflammation (colitis) in 100% of the animals [6]. The gut inflammation allows *S. tm* to out-compete the microbiota thus promoting pathogen overgrowth [21]. Here, we have extended this mouse model to study pathogen clearance at later phases of the primary infection when acute mucosal inflammation has ceased. We analyzed the levels of pathogen shedding, sIgA responses and the role of the microbiota. This revealed that the microbiota plays an essential role in pathogen clearance. The implications for curing asymptomatic excretors and preventing *S. tm* diarrhea are discussed.

Results

Sm-treated mice recover from *S. tm*^{att} induced gut inflammation and display extensive differences in the kinetics of fecal pathogen clearance

In sm-treated mice, infection with an attenuated *S. typhimurium* strain (*S. typhimurium* SL1344 *sseD*; termed *S. tm*^{att}; Table S1) is known to recapitulate key aspects of the early stages of human NTS diarrhea, i.e. gut inflammation 8h after orogastric exposure with infection confined to the gastrointestinal tract [22]. Symptoms of the acute gut inflammation usually decline by 5–7 days after infection [23]. In order to assess, if this model may be useful to dissect the role of pathogen-specific sIgA and the intestinal microbiota in pathogen clearance at the final stage of a primary infection we analyzed the outcome of long-term *S. tm*^{att} infections [6,24].

We monitored *S. tm*^{att} shedding for up to 60 days after infection. *S. tm*^{att} shedding in stool began to decrease after a few days, varied extensively between different animals and lasted for 2 to 8 weeks (Fig. 1A). At 60 day p.i., *S. tm*^{att} shedding was reduced below 10^5 cfu/g ($p<0.05$ day 1 vs. day 60 p.i.). At all stages, the infection remained largely confined to the gastrointestinal tract and draining mesenteric lymph nodes (MLN) and gut inflammation subsided after 7–44 days (Fig. 1B,C). Interestingly, we observed a high incidence of 'asymptomatic excretors' around day 44 post infection (p.i.). These mice were characterized by a low pathological score (≤ 3) and high cecum pathogen loads ($\geq 10^5$ cfu/g stool; Fig. 1C, right panel, green symbols). This may indicate that pathogen clearance from the gut lumen is not necessary in order to resolve gut inflammation. In fact, both might be independent from each other. We concluded that this model could be useful to analyze the mechanism of pathogen clearance from the gut lumen after infection.

S. tm^{att} induces O-antigen specific mucosal protection

Next, we wanted to address if mice that had experienced a primary *S. tm*^{att} infection in our model developed an adaptive immune response that would protect against gut inflammation upon re-infection with the same pathogen. This would be a prerequisite for functional analysis of antibody responses in pathogen clearance. Therefore, we extended the infection model as depicted in Fig. 2A ('immunization-challenge' protocol). Sm-treated mice were infected with *S. tm*^{att} for 39 days as in the standard protocol (= experimental group; mock-immunization = negative control). This allowed sufficient time for recovering from acute inflammation and the generation of a *S. tm*-specific adaptive immune response (Fig. 1C; see also Fig. 2C,D). At day 39, the mice were treated with ampicillin to transiently suppress the microbiota and eliminate any *S. tm*^{att} which may have persisted in the gut. We then

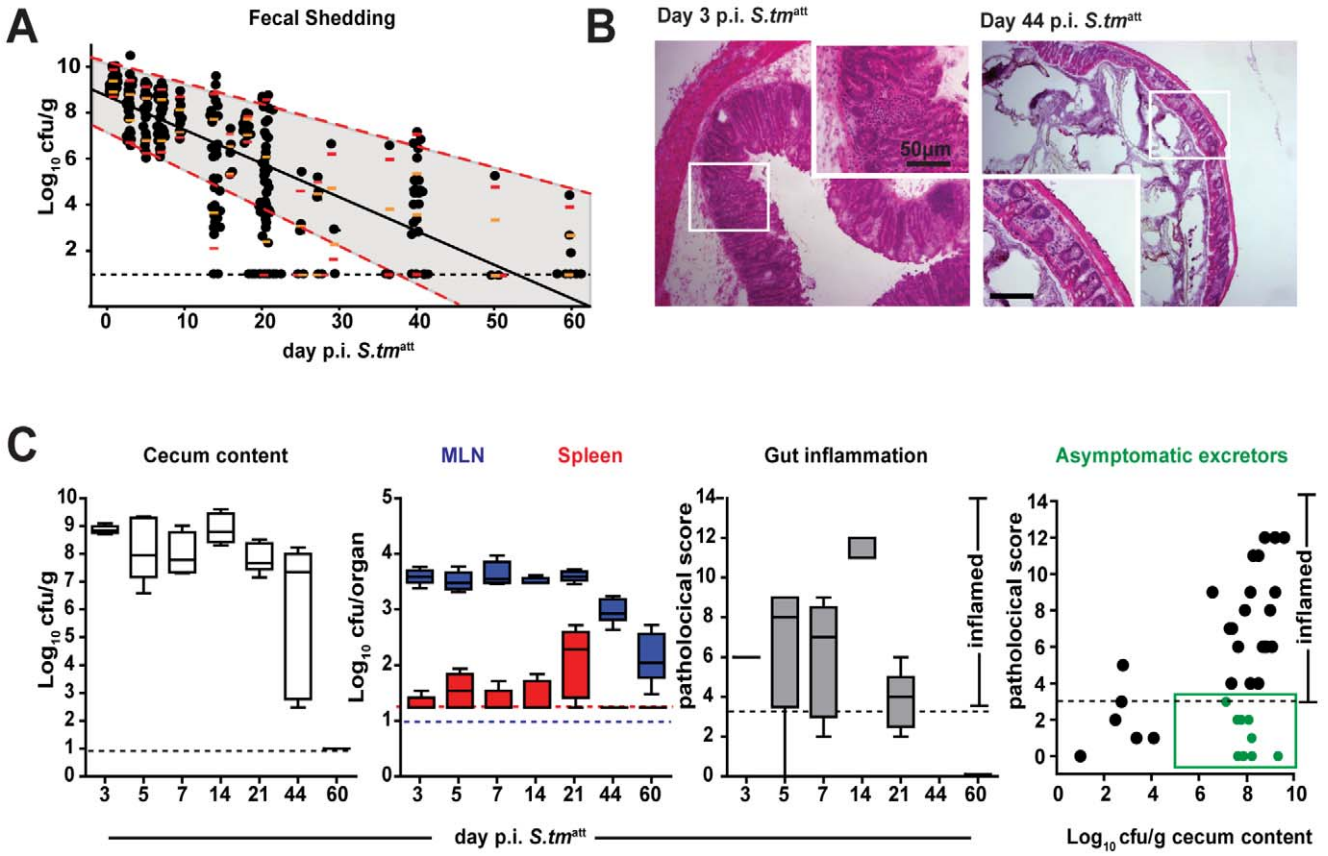


Figure 1. *S. tm*^{att} infection yields 'asymptomatic excretors' and elicits O-antigen specific immunity. A. Time course of fecal *S. tm*^{att} shedding. Sm-treated mice were infected with *S. tm*^{att} and fecal *Salmonella* shedding was monitored ($5<n<48$ individual mice per time point). Medians are shown in black; orange and red: 5%, 25%, 75% and 95% quantiles. Dashed red lines: weighted linear regression on the 5% and 95% quantiles. **B**. H&E stained cross-section of the cecum at day 3 (left) and day 44 (right) post *S. tm*^{att} infection. Enlarged section (white box) is shown in inset. Scale bar: 50µm. **C**. *S. tm*^{att} loads in cecum (left panel; Log_{10} cfu/g), spleen (red) and MLN (blue; both Log_{10} cfu/organ; 2nd panel) and cecal mucosa inflammation (3rd panel) at the indicated times post *S. tm*^{att} infection. 'Asymptomatic excretors' (4th panel) are defined as showing a pathological score ≤ 3 while shedding $\geq 10^5$ cfu/g *S. tm*^{att}.(green box). Each dot represents an individual mouse between day 3 and 60 *S. tm*^{att} immunization. Black dotted line: detection limit.
doi:10.1371/journal.ppat.1001097.g001

challenged the animals with wild type *S. typhimurium* (wt; ampicillin resistant; 200 cfu by gavage). In the mock-immunized mice, wt *S. typhimurium* efficiently colonized the gut and elicited acute intestinal inflammation within two days after challenge (Fig. 2B). In contrast, the *S. tm*^{att}-immunized mice were generally protected against wt *S. typhimurium*-inflicted disease (8/10 mice with cecal pathology score ≤ 3; $p = 0.0099$; Fig. 2B).

Bacterial surface structures and secreted proteins are dominant targets of adaptive immune responses [18,25,26,27,28,29]. Therefore, we analyzed whether surface-protein or O-antigen specific immune responses might explain the protection of *S. tm*^{att}-immunized mice. No protection was observed against challenge with the NTS serotype *S. enteritidis* (*S. en*^{wt}), harboring a different LPS-O-antigen, or an O-antigen deficient isogenic *S. typhimurium* mutant (*S. tm*$^{\Delta O}$; Δ*wbaP*; Table S1; $p>0.05$ vs. colitis in mock immunized controls). Thus, *S. tm*^{att}-immunized mice mounted an adaptive immune response which protected from mucosal disease on re-infection with the pathogen in an O-antigen-dependent way.

S. tm^{att} induces pathogen-specific sIgA

The exquisite O-antigen specificity of protection from a second round of inflammation suggested that adaptive immunity and particularly sIgA may be the crucial mechanism not only for preventing inflammation on re-infection, but also for clearing pathogens from the gut. Therefore, we determined the kinetics of the *Salmonella*-specific humoral immune response by measuring specific Ig via surface staining of live, intact bacteria by flow cytometric analysis (Fig. 2C). This assay accurately differentiates *S. tm* specific antibodies from antibodies directed against closely related species, such as *E. coli* [30] (Fig.S1A–C). *S. tm*-specific IgM, IgG and IgA were detectable in the serum as early as 7 days post immunization. By day 14, all mice secreted *S. tm* -surface-specific sIgA into the gut lumen. Mucosal sIgA responses were confirmed by immunohistochemistry (Fig.S2). *Salmonella* antigens targeted by this strong, specific humoral immune response were analyzed by Western blotting. The antibody response was indeed pathogen-specific, as *Lactobacillus reuteri* RR and *Enterococcus faecalis*, two commensals isolated from our mouse colony, were not recognized (Fig. 2D; Fig.S3). In analogy to the human infection (Fig.S4), the antibody response included sIgA recognizing the O-antigen of *S. tm* (protease resistant ladder-like bands in the Western blot; Fig. 2D), a highly repetitive sugar structure of the lipopolysaccharide (LPS), coating the surface of the pathogen. In contrast, the O-antigens from *S. enteritidis* and *E. coli*, which have a different sugar structure or LPS from the O-antigen deficient mutant *S. tm*$^{\Delta O}$ were not recognized. In addition, antibodies to several prominent

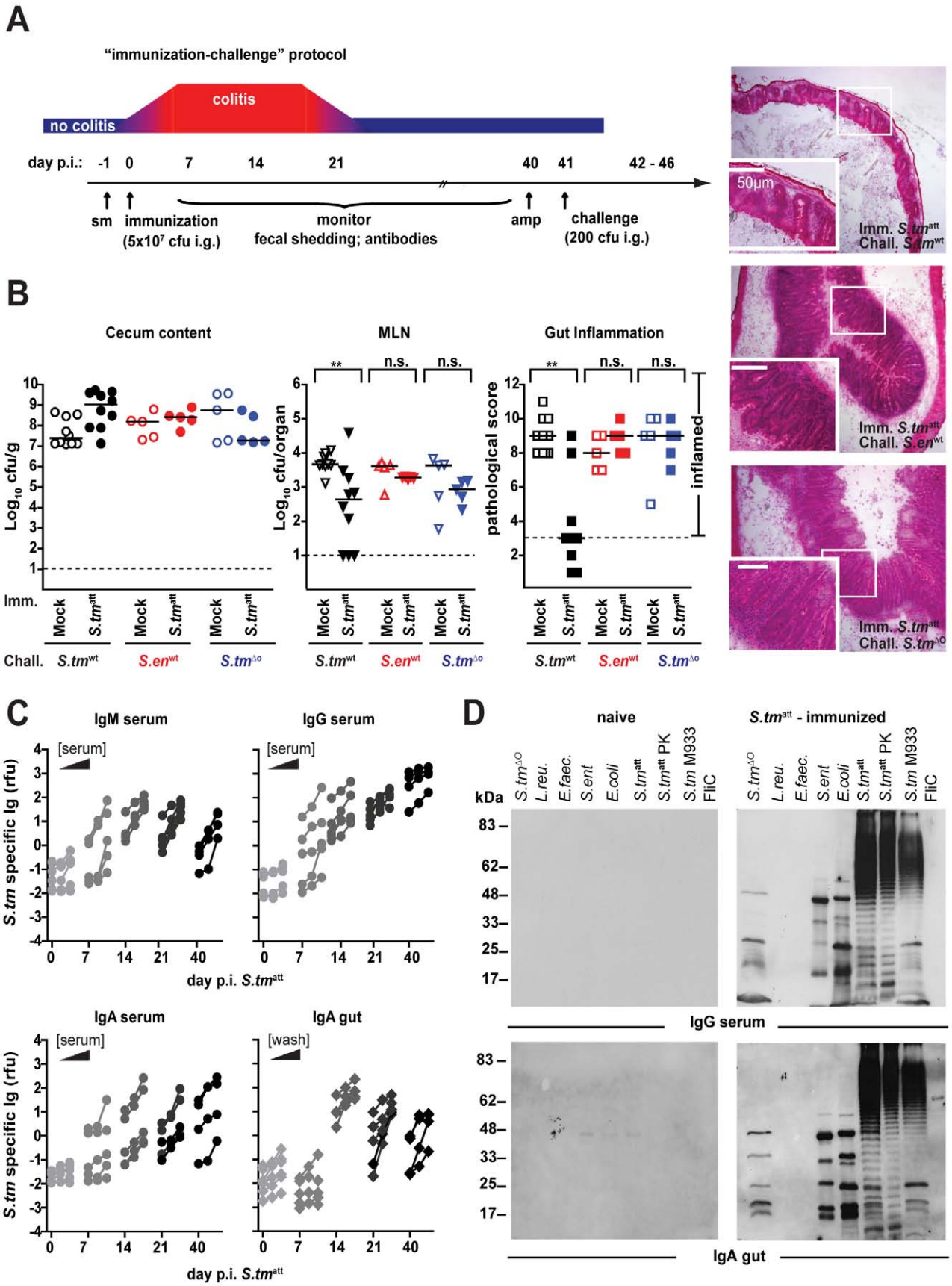

A
"immunization-challenge" protocol
colitis
no colitis
day p.i.: -1 0 7 14 21 40 41 42 - 46
sm
immunization (5x10^7 cfu i.g.)
monitor fecal shedding; antibodies
amp
challenge (200 cfu i.g.)
50µm
Imm. S.tm^att Chall. S.tm^wt
Imm. S.tm^att Chall. S.en^wt
Imm. S.tm^att Chall. S.tm^Δo
B
Cecum content
MLN
Gut Inflammation
Log10 cfu/g
Log10 cfu/organ
pathological score
inflamed
**
n.s.
n.s.
Imm.
Mock
S.tm^att
Chall.
S.tm^wt
S.en^wt
S.tm^Δo
C
IgM serum
IgG serum
IgA serum
IgA gut
[serum]
[wash]
S.tm specific Ig (rfu)
day p.i. S.tm^att
D
naive
S.tm^att - immunized
kDa
S.tm^ΔO
L.reu.
E.faec.
S.ent
E.coli
S.tm^att
S.tm^att PK
S.tm M933
FliC
83
62
48
33
25
17
IgG serum
IgA gut

Figure 2. *S. tm*^{att} induces O-antigen specific mucosal protection. A. 'Immunization-challenge' model. At day 0, sm-treated mice are infected and *S. tm*^{att} (5×10^7cfu; i.g.). They develop enteric pathology (red) that usually declines by day 14–20 p.i. (blue). Afterwards, the mice appear healthy. At day 40 p.i., mice are treated with ampicillin (20mg i.g.) and challenged with *S. tm*^{wt} (or other strains; 200cfu i.g.). The degree of *Salmonella*-induced gut inflammation and pathogen loads are determined at day 1–5 post challenge. **B**. *S. tm*^{att} immunized mice are protected in an O-antigen dependent fashion. *S. tm*^{att} (filled symbols) or mock (open symbols) immunized mice were challenged with *S. tm*^{wt} (black; n = 10), *S. en*^{wt} (red circles; n = 5) or *S. tm*$^{\Delta O}$ (blue; n = 5) at day 40 post immunization. At day 2 post challenge, challenge strain loads were assessed in the cecum content (left panel) and the MLN (middle panel). Dashed lines indicate detection limits. Right panels: inflammation of the cecal mucosa (score$\leq$3 indicates no inflammation). Black bar: median; *p$<$0.05; **p$<$0.005; n.s. = not significant. H&E stained cross-sections of the cecum of *S. tm*^{att}-immunized mice at day 2 post challenge with *S. tm*^{wt} (upper panel), *S. en*^{wt} (middle panel) and *S. tm*$^{\Delta O}$ (lower panel). Enlarged section (white box) is shown in the lower panel. Scale bar: 50μm. **C**. Time course of the *S. tm*^{att} specific humoral immune response. Antibodies directed against the surface of *S. tm*^{att} in serum or gut wash of the *S. tm*^{att} -immunized mice from Fig. 1C were analyzed by bacterial FACS (Materials and Methods; Fig.S1). The Y-axis shows *S. tm*^{att} specifc Ig (relative fluorescence units; rfu), the X-axis different dilutions of serum or gut wash (1: 20, 1:60, 1:180) at different days post *S. tm*^{att} immunization. **D**. *S. tm*^{att}-immunized mice mount an O-antigen specific antibody response. Serum and gut wash Ig from naïve and *S. tm*^{att} infected mice (day 40 post infection) were analyzed by immunoblot against different bacterial lysates (*S. tm*$^{\Delta O}$; *L. reuteri*; *E. faecalis*; *S. ent*^{wt}; *E. coli*; *S. tm*^{att}; *S. tm*^{att} digested with proteinase K; *S. tm* M933 [no flagella, no functional TTSS]; flagellin FliC). Ig was detected with the respective *HRP*-labeled secondary antibodies. The experiment is representative for 6 different animals.
doi:10.1371/journal.ppat.1001097.g002

protein antigens were detected. Most of these protein antigens were conserved in different *Salmonella* and *E. coli* strains, but not in *L. reuteri* RR or *E. faecalis*.

It should be noted that acute mucosal inflammation seems necessary to elicit immune responses protecting from enterocolitis. It was also shown previously, that invasive *Salmonella* strains triggered more potent adaptive immune responses [31]. Mice not pretreated with sm before immunization (low antigen loads, no gut inflammation), sm-treated mice immunized with *S. tm*^{avir} (high antigen loads, no gut inflammation) and parenterally immunized mice (*S. tm*^{att} i.v.; systemic antigen loads, no gut inflammation) did not mount detectable levels of O-antigen-specific sIgA. None of the mice were protected against wild type *S. tm* (*S. tm*^{wt}) mediated enteropathogenesis (Fig.S5).

Overall, these data demonstrated that the LPS O-antigen was the dominant protective antigen and that mice mount a robust pathogen-specific sIgA response during the first round of infection. This is in line with earlier data from studies in the mouse typhoid fever model, in chicken and data from human patients [18,25,26,27] (Fig.S4). However, from these first sets of experiments we could not conclude whether pathogen-specific sIgA was sufficient for *S. tm* clearance from the gut.

sIgA is dispensable for pathogen clearance from the gut lumen

In order to address sIgA functions in pathogen clearance, we analyzed the outcome of *S. tm*^{att} infection in different KO-mice lacking key mediators of functional adaptive immune responses. We determined whether T-cell dependent or -independent mucosal sIgA immune responses [30,32,33] were critical for termination of inflammation, pathogen clearance and protection from inflammation on re-infection. 'Immunization-challenge' experiments were performed on mice lacking the T-cell receptor (TCR$\beta^{-/-}\delta^{-/-}$; T-cell deficient), B-cells ($J_H^{-/-}$), IgA ($IgA^{-/-}$) or sIgA and sIgM-transport into the gut lumen ($pIgR^{-/-}$; Table S2). Two days after initial infection with *S. tm*^{att}, all knockout mice displayed pronounced gut inflammation (data not shown) and gut inflammation subsided by day 40 (Table 1). This demonstrated that the acute mucosal inflammation can be efficiently terminated in the absence of T-cells, B-cells, antibodies or sIgA. Furthermore, several $IgA^{-/-}$ (3/4) and $pIgR^{-/-}$ (2/5) animals managed to clear *S. tm*^{att} from the gut lumen by day 40 p.i. This indicated that pathogens can (at least in some cases) be cleared from the gut lumen, in the absence of pathogen-specific sIgA (and sIgM) in the gut lumen. In order to exclude differences attributable to alterations in microbiota composition between different mouse lines, we have compared the *S. tm*^{att} clearance kinetics between $IgA^{-/-}$ and wild type littermates ($IgA^{+/-}$, $IgA^{+/-}$, $IgA^{+/+}$; Fig. 3). This verified that kinetics of pathogen clearance was not affected by presence or absence of sIgA.

Strikingly, none of the *S. tm*^{att} -immunized knockout mice developed O-antigen specific antibodies and none were protected from intestinal inflammation upon challenge with *S. tm*^{wt} (pathological score $\gg$3; Table 2 and Fig.S6). Thus, a T-cell

Table 1. Primary infection with *S. tm*^{att}.

Mouse line*	day 2	day 40						
	Gut inflam.‡	Cecum cont. (cfu/g)	MLN (cfu/organ)	Spleen (cfu/organ)	Gut inflam.‡	Antibodies		
						Serum IgG	Serum IgA	sIgA
wt	+	10	625	60	0	++	++	++
TCR$\beta^{-/-}/\delta^{-/-}$	+	6×10^7	40	20	2	+#	+#	+#
$J_H^{-/-}$¤	+	2×10^3¤	60¤	20¤	0¤	−¤	−¤	−¤
$IgA^{-/-}$	+	$10^{\text{✓}}$	1×10^3	20	1	++	−	−
$pIgR^{-/-}$	+	120§	1000	20	1	++	++	−

*median values of 4 or 5 mice per group; pathogen loads: cfu of *S. tm*^{att}.
‡pathology score.
*median values of 4 or 5 mice per group.
#no LPS specific Ig.
✓3/4 $IgA^{-/-}$ mice had no detectable *S. tm*^{att} in the gut lumen.
§2/5 $pIgR^{-/-}$ mice had no detectable *S. tm*^{att} in the gut lumen.
¤$J_H^{-/-}$ day 60 post *S. tm*^{att} immunization.
doi:10.1371/journal.ppat.1001097.t001

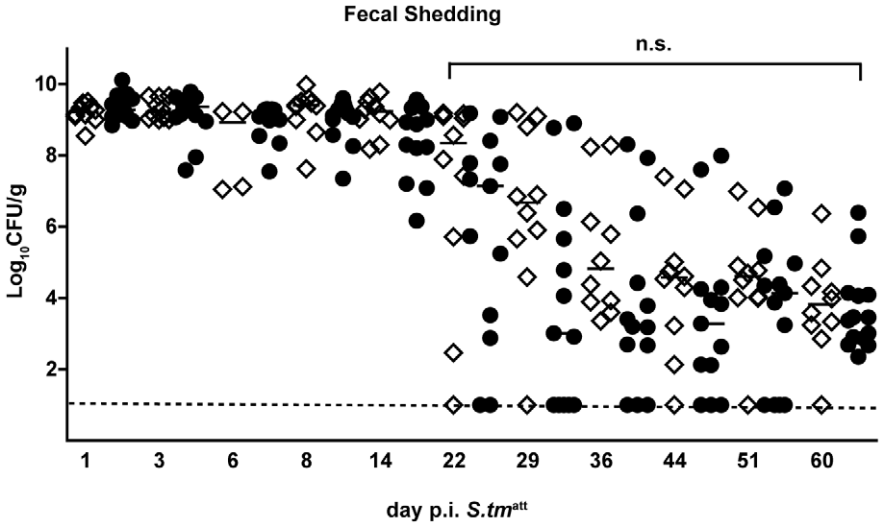


Figure 3. IgA deficiency does not affect kinetics of pathogen clearance. Time course of fecal *S. tm*^{att} shedding in IgA$^{-/-}$ and IgA-proficient littermates. IgA$^{-/-}$ and IgA-proficient littermates were generated by crossing IgA$^{+/-}$ mice in order to yield littermates with comparable gut flora. Sm-treated IgA$^{-/-}$ (n = 10; white diamonds), IgA$^{+/-}$ (n = 7; black circles) and wild type (n = 7; black circles) littermates were infected with *S. tm*^{att} and fecal *Salmonella* shedding was monitored until day 60 post infection. Black bar: medians. Dashed line: detection limit. Statistics: comparison of fecal shedding by IgA$^{-/-}$ vs. IgA$^{+/-}$ and IgA$^{+/+}$ (n.s.: $p>0.05$).
doi:10.1371/journal.ppat.1001097.g003

dependent, adaptive mucosal sIgA response is essential for protection from secondary disease, but is dispensable for resolving the initial inflammatory response to *S. tm*^{att} and for clearing the pathogen from the intestinal lumen.

sIgA restricts intestinal pathogen growth and mucosal access

Though dispensable, our findings did not exclude that sIgA exerts an effector function [34] which contributes in some way to pathogen clearance. To identify such mechanisms, we analyzed the effects of sIgA on pathogen growth and its interaction with the host's intestinal mucosa in greater detail. First, we applied a modified 'immunization-challenge' protocol. Sm-treated mice were infected with *S. tm*^{att}, an equivalent *S. enteritidis* strain (*S. en*^{att}; *S. enteritidis* 125109 *sseD*; [35]) or mock. Antibody responses and *S. tm*^{att}/ *S. en*^{att} loads in the stool were monitored (Fig.S7 and data not shown). After 39 days, immunized mice were treated with ampicillin (elimination of microbiota and remaining *S. tm*^{att} or *S. en*^{att}) and challenged with a 1:1 mixture of *S. tm*^{avir} and *S. en*^{avir} (ampicillin resistant; *sseDinvG* mutants; 200 cfu each by gavage; Table S1). These latter mutants can colonize the gut lumen of naïve mice for up to four days, remain confined to the gastrointestinal tract and they do not elicit enteropathogenesis, thus mimicking the situation in the intestines of 'asymptomatic excretors' [21,24]. We decided not to use *S. tm*$^{\Delta O}$ for this type of competition experiments as it displays a pronounced competitive growth defect in mice when co-infections are performed with an isogenic wild type strain [36]. In the gut lumen of *S. tm*^{att} immunized mice, *S. en*^{avir} out-competed *S. tm*^{avir} (Fig. 4A; black symbols). In *S. en*^{att} immunized mice, *S. tm*^{avir} out-competed *S. en*^{avir} (red symbols), and in mock-immunized mice, both strains colonized with equal efficiency. Therefore, O-antigen specific sIgA may help controlling pathogen growth or survival in the gut lumen. Furthermore, *S. tm*^{avir} (but not *S. en*^{avir}) was aggregated in the gut lumen and occluded from the mucosal surface of *S. tm*^{att} immunized mice (Fig. 4A, right panels). Pathogen occlusion was confirmed by assessing pathogen loads in the gut tissue of challenged mice. In *S. tm*^{att} -immunized animals, *S. tm*^{wt} tissue

Table 2. Challenge infection (day 2 post *S. tm*^{wt} challenge).

Mouse line*	naïve mice				*S. tm*^{att} immunized mice			
	Gut inflam.‡	Cecum cont. (cfu/g)	MLN (cfu/organ)	Spleen (cfu/organ)	Gut inflam.‡	Cecum cont. (cfu/g)	MLN (cfu/organ)	Spleen (cfu/organ)
wt	9	2×10^7	4×10^3	240	3	3×10^7	7×10^2	60
TCR$\beta^{-/-}/\delta^{-/-}$	10	1×10^7	8×10^3	290	8	4×10^8	1×10^1	280
$J_H^{-/-}$	9	2×10^7	3×10^3	20	8	5×10^8	3×10^2	20
IgA$^{-/-}$	8	8×10^7	4×10^3	30	8	2×10^9	1×10^3	20
pIgR$^{-/-}$	9	2×10^7	2×10^3	20	9	1×10^7	2×10^3	20

*median values of 4 or 5 mice per group; pathogen loads: cfu of *S. tm*^{wt} (B).
‡pathology score.
*median values of 4 or 5 mice per group.
¤$J_H^{-/-}$ day 60 post *S. tm*^{att} immunization.
doi:10.1371/journal.ppat.1001097.t002

loads were 100-fold lower than in mock-immunized controls (Fig. 4B). In contrast, *S. tm*^{att} immunization did not prevent the invasion of *S. enteritidis*. Furthermore, *S. tm*^{att} immunized pIgR$^{-/-}$ mice, which cannot transport sIgA across the gut epithelium, failed to prevent gut tissue invasion by wt *S. typhimurium* into the mucosal tissue (Fig. 4B). Thus, the O-antigen-specific sIgA response conferred protection by restricting pathogen growth in the gut lumen and preventing the interaction of the pathogen with the intestinal mucosa. To some extent, this may also contribute to pathogen clearance from the gut lumen.

Mice harboring a low-complexity microbiota become long-term asymptomatic excretors

While O-antigen-specific sIgA was indispensable to prevent disease, it did not seem to be a major determinant in pathogen clearance from the gut lumen. The onset of adaptive sIgA responses and cessation of symptoms seemed to occur well ahead of *S. tm*^{att} elimination from the intestines. Moreover, IgA deficiency did not affect pathogen clearance kinetics (Table 1; Fig. 3). This was different from most well studied paradigms of acute systemic infection where the onset of protective immunity coincides with declining pathogen loads. This strongly suggested that sIgA-independent mechanisms may underlie pathogen clearance from the gut.

Thus, we hypothesized that the microbiota might play a crucial role in pathogen clearance. The microbiota is a dense bacterial community composed of approx. 500–1000 different species [9,37]. It confers numerous beneficial effects to the host [38] including 'colonization resistance', i.e. a generalized interference with the growth of many pathogens in the gut of a naïve host [3]. Antibiotic treatment disrupts the normal microbiota, alleviates colonization resistance and constitutes a known risk factor for *Salmonella* infections in humans and mice [7,9,10,21,39]. Furthermore, the species composition of the microbiota - and by inference the degree of colonization resistance - can vary significantly between different individuals [40]. Therefore, the microbiota composition might explain why *Salmonella* shedding by 'asymptomatic excretors' can last for months or years.

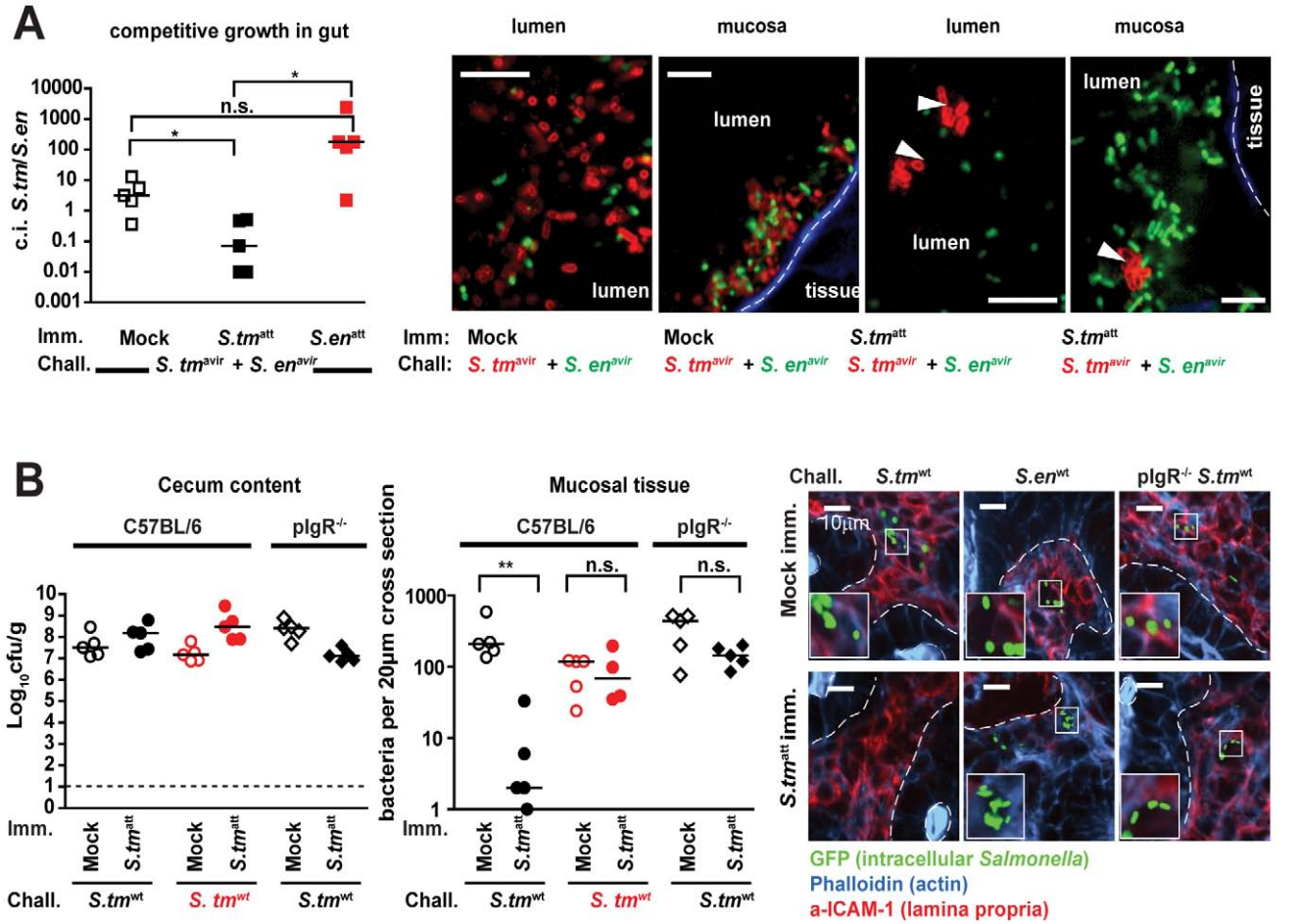


Figure 4. Immunization elicits O-antigen specific sIgA which retards pathogen growth and restricts mucosal access. A. sIgA retards pathogen growth and occludes mucosal access. Mice were immunized with *S. tm*^{att}, *S. en*^{att} or mock (n = 5 per group), treated with ampicillin and challenged for 1 day with a 1:1 mixture *S. tm*^{avir}(amp^{R}; pWKS30) and *S. en*^{avir} (amp^{R}; pM979-GFP^{+}). None of the mice developed gut inflammation. Left panel: competitive index (c.i.) of *S. tm*^{avir}(amp^{R}; pWKS30) and *S. en*^{avir} (amp^{R}; pM979-GFP^{+}) in the cecal lumen. Right panels: Immunofluorescence microscopy of the cecal lumen (left panels) and the mucosal surface (right panels; actin brush boarder = blue) to detect *S. tm*^{avir} (red α-*S. tm* LPS stain) and *S. en*^{avir} (green GFP^{+}). Scale bar: 10µm. **B**. sIgA blocks mucosal invasion by *S. tm*^{wt}. C57Bl/6 (circles) or pIgR$^{-/-}$ mice (diamonds) were immunized with mock (open symbols) or *S. tm*^{avir} (closed symbols) and challenged with *S. tm*^{wt} (black) or *S. en*^{wt} (red). Bacterial loads in the cecal lumen (left) and *Salmonella* invasion into the mucosal tissue (middle) was determined at 2 days post challenge. Right panels: Immunofluorescence microscopy of GFP-expressing *S. tm*^{wt} or *S. en*^{wt} (green) in the cecal mucosa (red: ICAM-1, lamina propria; blue: Actin, epithelial brush border); White dotted lines mark epithelial-submucosal boarder; Scale bar: 10µm.
doi:10.1371/journal.ppat.1001097.g004

In sm-treated mice, the microbiota is transiently reduced, but rapidly returns to pretreatment community composition, re-establishes 'colonization resistance' and 'asymptomatic excretion' occurs just transiently (Fig. 1C; [21,41]). For this reason, our original infection model was not optimally suited for dissecting the differential role of the microbiota and sIgA in pathogen clearance.

To overcome this problem we used 'L-mice' which harbor a well defined, low complexity microbiota (L = 'LCM mice'; [20]). L -mice are ex-germ free mice that are stably associated with the 'Altered Schaedler Flora' [42] comprising <20 species. The representatives with the highest abundance are ASF500 (Firmicutes; Clostridia; Clostridiales; Lachnospiraceae; unclassified_Lachnospiraceae) and ASF519 (Bacteroidetes; Bacteroidia; Bacteroidales; Porphyromonadaceae; Parabacteroides). Thus, the L microbiota resembles the conventional (C) microbiota of mice and men at broad lineages levels [43]. However, in spite of an equally high bacterial density as the C microbiota, the L microbiota does not confer colonization resistance [20]. Accordingly, *S. tm*^{att} efficiently colonized the gut lumen of L-mice at high levels ($\geq 10^8$cfu/g) and elicited pronounced enteropathogenesis by day 2 p.i. even without previous antibiotic treatment (Fig. 5A). After 40 days, all immunized L-mice had resolved acute inflammation, but kept on shedding *S. tm*^{att} at high levels for at least 83 days (Fig. 5A; see also below). This was not due to a defective O-antigen-specific sIgA response: sIgA responses in L-mice were as pronounced as in C-mice as indicated by the increased numbers of IgA$^+$ cells in the cecal mucosa (Fig. 5B,C and Fig.S2) and by Western Blot analysis (Fig.S8 and Fig 2D). The strong adaptive mucosal immune response was also confirmed by gene expression profiling of the cecal mucosa (Fig. 5D, Fig.S9, Table S3). Furthermore, challenge experiments confirmed the O-antigen-specific protection from enteropathogenesis (Fig. 6). However, despite this O-antigen-specific sIgA response, high-level pathogen shedding persisted in all analyzed animals (Fig. 5A; see also below). Therefore, O-antigen-specific sIgA was insufficient for luminal *S. tm*^{att} clearance. This was in line with our hypothesis that elements of the normal, complex microbiota (which is lacking in L-mice) may play a key role in terminating fecal *S. tm*^{att} shedding.

Transfer of a complex microbiota facilitates pathogen clearance

To formally define the importance of the commensal microbiota in pathogen clearance, two groups of L-mice were infected with *S. tm*^{att} for 83 days. The first group was kept under strict hygiene isolation and shed high loads of *S. tm*^{att} until the end of the experiment (*S. tm*^{att}→L; Fig. 7A; open symbols). The second group was exposed to C microbiota at day 40 by placing C donor mice into the same cage (*S. tm*^{att}→L/C; 6 independent cages). Both groups of mice developed the typical pathogen-specific, adaptive sIgA response by day 83 p.i. (Fig. 7B,C). Upon introduction of the C donor mice, fecal shedding decreased gradually and ceased in most of the *S. tm*^{att}→L/C mice by day 83 ($<10^5$cfu/g; Fig. 7A; black symbols) but not in the *S. tm*^{att}→L group. This suggested that pathogen clearance was mediated in some way by the complex microbiota.

In order to verify microbiota-transfer, we assessed microbiota composition using high-throughput 16S rRNA gene sequence analysis (Materials and Methods). *S. tm*^{att}→L/C mice displayed significantly higher diversity than *S. tm*^{att}→L mice as well as LCM mice at day 2 and 40 after *S. tm*^{att} immunization (Fig. 7D). The rarefaction curves indicated that *S. tm*^{att}→L/C mice had acquired a microbiota of the similar complexity as the C donor mice. This was confirmed by assessing the richness (actual diversity) of the samples by calculating the Shannon index (H) and species evenness (E) as well as the Chao1 diversity estimate (Table S4). Accordingly, the taxonomy assignment confirmed that the number of bacterial taxa in the stool increased significantly in *S. tm*^{att}→L/C mice. All *S. tm*^{att}→L mice carried high loads of *Enterobacteriaceae* (i.e. *Salmonella* spp., *E. coli* spp.; red colors) in their stools. In contrast, no *Enterobacteriaceae* were detected in the stools of 3 (out of 6) *S. tm*^{att}→L/C mice and the remaining 3 animals carried low levels of this family (yellow colors, Fig. 7E). In addition, the microbiota composition was similar between all *S. tm*^{att}→L/C animals as demonstrated by hierarchical cluster analysis of eubacterial family profiles (Fig. 7E). This indicated that pathogen displacement occurs in a reproducible, stereotypic fashion and may not result from random transfer of only few members of the conventional microbiota. Most importantly, these data demonstrate that members of the conventional microbiota can upon transfer lead to the termination of sustained pathogen shedding in L-mice.

It remained unclear whether pathogen clearance was mediated directly by the microbiota or by microbiota-induced mucosal responses. Recently, it has been shown that parts of the microbiota (i.e. segmented filamentous bacteria) induce mucosal TH-17 cell responses that can protect from pathogen infection [2]. However, we did not observe differences in IL-17A or IFN gamma-producing CD4 T-cells in the MLN of *S. tm*^{att}→L and *S. tm*^{att}→L/C animals by day 83 (Fig. 8). Furthermore, we tested if total MLN cells obtained from *S. tm*^{att}→L/C animals would, upon transfer into *S. tm*^{att}→L (d.40) induce clearance of intestinal *S. tm*^{att}. However, this was not the case (Fig.8). This was in line with the notion that the microbiota may directly mediate pathogen clearance.

Discussion

In this study, we have defined the contributions of sIgA and the microbiota in protecting the host from NTS infection. During the first encounter with the pathogen, the microbiota mediates at least two different protective functions, colonization resistance and pathogen clearance. The former is well established and prohibits the growth of diverse incoming pathogens, thus preventing colonization right on [3,5,20,44]. Here, we identified pathogen clearance as a second protective function attributable to the microbiota. Pathogen clearance eliminates the pathogen from the gut lumen after an episode of acute infection, i.e. after *Salmonella* diarrhea. This differs from colonization resistance as the pathogen starts out at high density and the normal microbiota must re-grow from a state of depletion and disturbed composition (i.e. caused by the pathogen and the inflammatory response). Compared to the microbiota, an adaptive sIgA response mounted during the later stages of an acute infection contributes little to clearing the pathogen from the gut lumen. However, pathogen-specific sIgA protects from mucosal inflammation if the same pathogen is encountered for a second time. Thus, the microbiota and sIgA have complementary functions which jointly protect against enteropathogenic bacteria during the initial infection and subsequent exposure.

How does the microbiota mediate pathogen clearance? The lack of suitable assay systems has hampered addressing this question in the past. Clearly, *S. tm* clearance starts out in a situation where the pathogen has grown up in the gut lumen, inflicted disease and thereby slashed microbiota density, composition and/or function [45]. This situation is gradually reversed, involving the decrease of luminal pathogen loads as well as microbiota re-growth. Finally, normal microbiota composition, density and function are restored. Conceivably, some of the

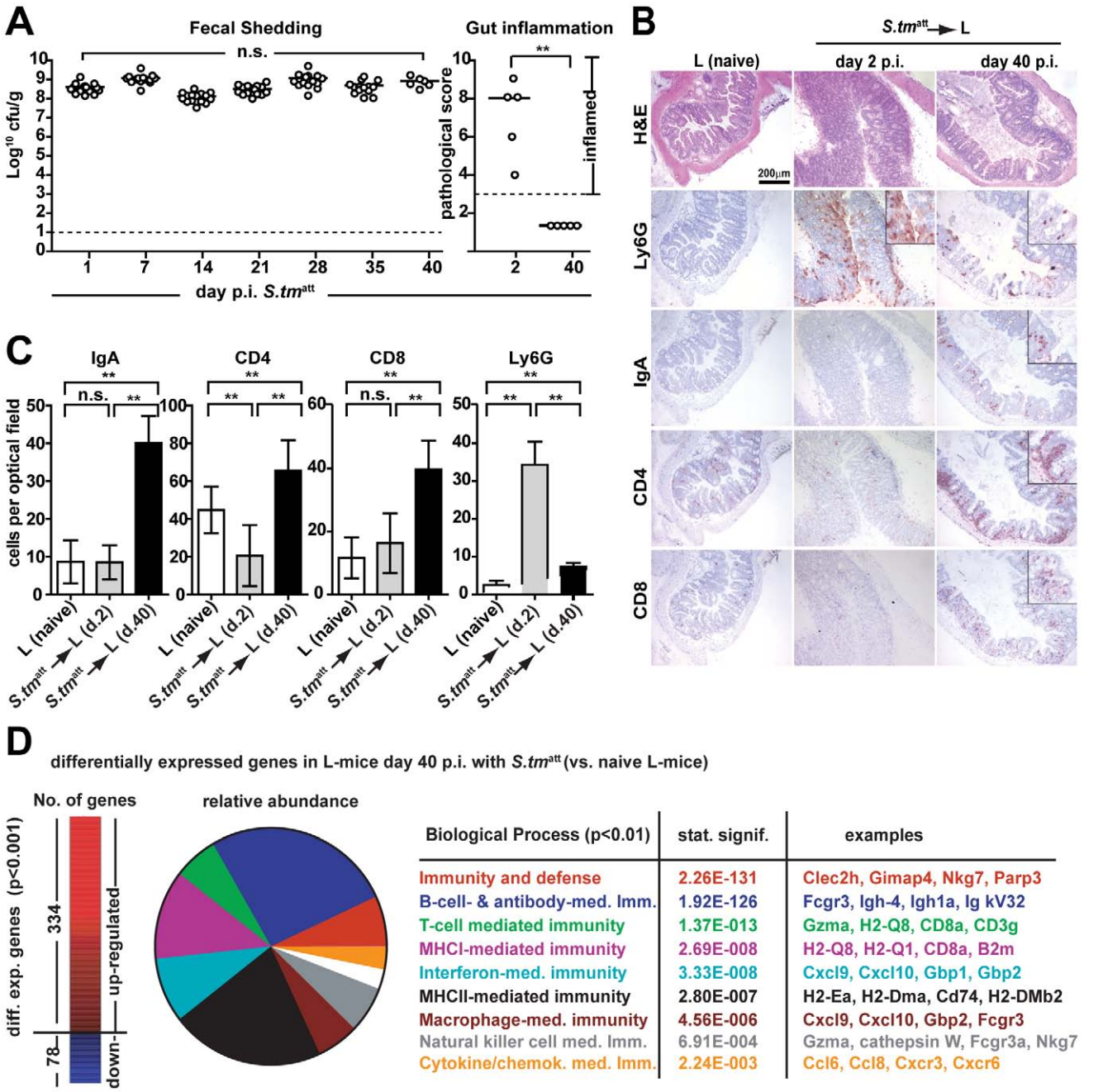


Figure 5. An O-antigen-specific sIgA response is insufficient to terminate *S. tm*^{att} shedding by L-mice. A. L-mice do not clear *S. tm*^{att} from the gut. L-mice (n = 15) were immunized with *S. tm*^{att} (no streptomycin-treatment) and fecal shedding was monitored for 40 days (left panel). Gut inflammation was analyzed at day 2 and day 40 p.i. (5 mice per time point; right panel). **B. and C**. L-mice mount a pronounced adaptive mucosal immune response. Cecal tissue of naïve L-mice and L-mice at days two and 40 p.i. was stained by immunohistochemistry for Ly6G (granulocytes), IgA, CD4 (T-cells) and CD8 (T-cells) cellular markers. Quantitative data were from 15 randomly selected 40× high power fields (hpf) from 3–5 mice per group. Y-axis: average cell number per 40× hpf (**C**). **D**. Gene expression analysis of naïve and L-mice at day 40 post *S. tm*^{att} immunization. Left: Numbers of differentially expressed genes in *S. tm*^{att}-immunized L-mice. Middle: relative abundance of biological pathways significantly upregulated in *S. tm*^{att}-immunized L-mice. Processes, p-values and characteristic examples are shown as a table (right).
doi:10.1371/journal.ppat.1001097.g005

mechanisms conferring colonization resistance, i.e. bacteriocin production, inhibitory metabolites, oxygen depletion, receptor blocking, stimulating mucin- or antimicrobial peptide release, stabilization of the mucosal barrier, improvement of gut motility and/or nutrient limitation [5], might also contribute to different phases of pathogen clearance. Also, microbiota-mediated stimulation of the mucosal cellular immune system may be involved [2,46] even though TH-17 mediated responses do not seem to contribute significantly to *S. tm* clearance, as indicated by adoptive transfer experiments (Fig. 8). The mechanisms mediating clearance and the relative importance of the microbiota, sIgA and other mucosal immune responses may differ between different pathogens or even between different strains of a given pathogen. Identifying the commensal species (or consortia) involved and the

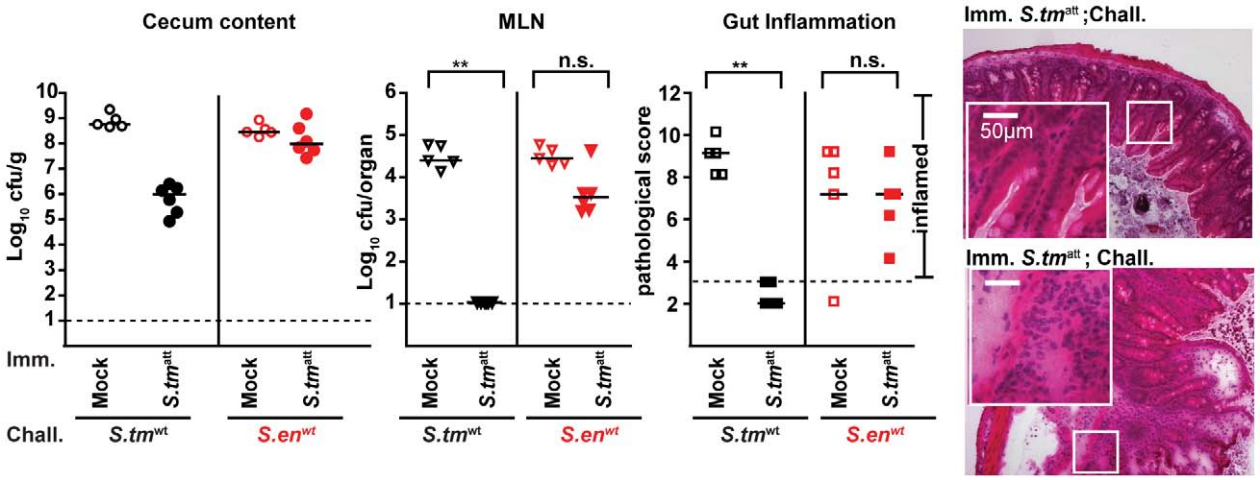


Figure 6. O-antigen specific protection from enteropathogenesis of *S. tm*^{att}-immunized L-mice. *S. tm*^{att}- (filled symbols) or mock- (open symbols) immunized mice were challenged for two days with *S. tm*^{wt} (black; n = 10) or *S. en*^{wt} (red circles; n = 5) at day 40 post immunization. Challenge-strain loads in the cecal content (left panel) and the MLN (middle panel) and cecal inflammation were assessed at day 2 post challenge. Dashed lines: detection limit or limit defining the absence of disease (pathological score ≤3). Black bars: median; *p<0.05; **p<0.005; n.s. = not significant. Right: H&E stained cross-sections of the cecum of *S. tm*^{att}-immunized L-mice at day two post challenge with *S. tm*^{wt} (upper panel) or *S. en*^{wt} (lower panel). Scale bar: 50µm.
doi:10.1371/journal.ppat.1001097.g006

molecular mechanisms mediating pathogen clearance will be an important task for future research.

Does sIgA contribute to pathogen clearance? Pathogen specific sIgA is produced by wild type animals during the phase of pathogen clearance. O-antigen-specific sIgA led to aggregation of luminal pathogens, prevented access to the enterocyte surface and reduced net pathogen growth as indicated by a reduced competitive index. Surprisingly, this had little effect on *S. tm* clearance. Wild type mice and IgA$^{-/-}$ littermates displayed equivalent rates of pathogen clearance. Moreover, sIgA did not reduce pathogen loads in the stool, at least in the L-mice in the absence of a complex gut flora. Thus, for pathogen clearance at the end of a primary enteric *S. tm* infection, a pathogen-specific sIgA response is neither necessary nor sufficient.

Instead, sIgA protected from mucosal inflammation upon re-infection with the same pathogen. The LPS O-antigen was the key protective antigen of this adaptive immune response. Protection was attributable to pathogen-aggregation in the gut lumen, reduced net pathogen growth and pathogen-exclusion from the epithelial surface, thus inhibiting pathogen invasion into the gut tissue. This required sIgA transport into the gut lumen, as immunized pIgR$^{-/-}$ mice, which fail to transport sIgA across the intestinal epithelium, have equivalent pathogen loads in the gut mucosa as non-immunized littermates or wild type animals. Thus, pathogen specific antibodies do not seem to contribute much to protection, once *S. tm* has breached the mucosal barrier. This is in line with earlier work on the roles of antibody responses in systemic *S. tm* infection [17,47]. In conclusion, our experiments show that O-antigen-specific sIgA responses protect against *Salmonella*-mediated gut inflammation upon re-infection.

It is interesting to consider the protective function of sIgA and the microbiota from an evolutionary perspective. The intestines of most animals are colonized by bacterial communities [43]. It seems safe to assume that microbiota have an evolutionary ancient function in protecting from infection. We speculate that this pertains to colonization resistance and to pathogen clearance and that both have evolved to provide protection against a broad range of pathogens. The elaborate adaptive immune system of modern mammals, including sIgA responses, evolved much later. It evolved in the presence of the protective functions provided by the microbiota, i.e. colonization resistance and pathogen clearance. The high efficiency of this microbiota-mediated protection may explain why sIgA responses have not evolved to affect the first round of infection with a given pathogen. This was simply not necessary. In contrast, evolving the sIgA response to protect in the case of repeated exposure to the same pathogen may have represented a strong benefit which cannot be accomplished by the microbiota. This evolutionary history may explain why the sIgA response contributes little during the primary infection. Anyhow, in modern mammals the microbiota and sIgA have quite different protective functions which complement each other during the initial- and subsequent encounters with a given pathogen.

An 'unfavorable' microbiota composition, e.g. in L-mice, can result in long term shedding. Asymptomatic NTS excretion is also observed in humans recovering from acute diarrhea. This period of asymptomatic excretion normally lasts for two to eight weeks, but may last for more than a year in a few patients. This poses a risk of transmission. In analogy to the long term shedding by L-mice, we propose that these individuals might lack some unidentified component of the normal microbiota. In L-mice, the pathogen is cleared upon transferring microbiota from a healthy donor. This may have implications for managing human long term asymptomatic excretors. Traditionally, patients are advised to adhere to strict personal hygiene and might even be isolated in order to reduce the risk of transmission. However, at the same time this deprives the patients from exposure to conventional microbiota from healthy individuals which might enhance pathogen clearance. So far, we do not know the species of the microbiota, the cellular interactions, and molecular mechanisms explaining pathogen clearance. However, the experimental systems presented in our study may provide the tools to address these important issues. Our findings provide a basis for future research on optimal management of 'asymptomatic excretors', NTS vaccine development and microbiota-directed therapy for acute diarrheal NTS infections.

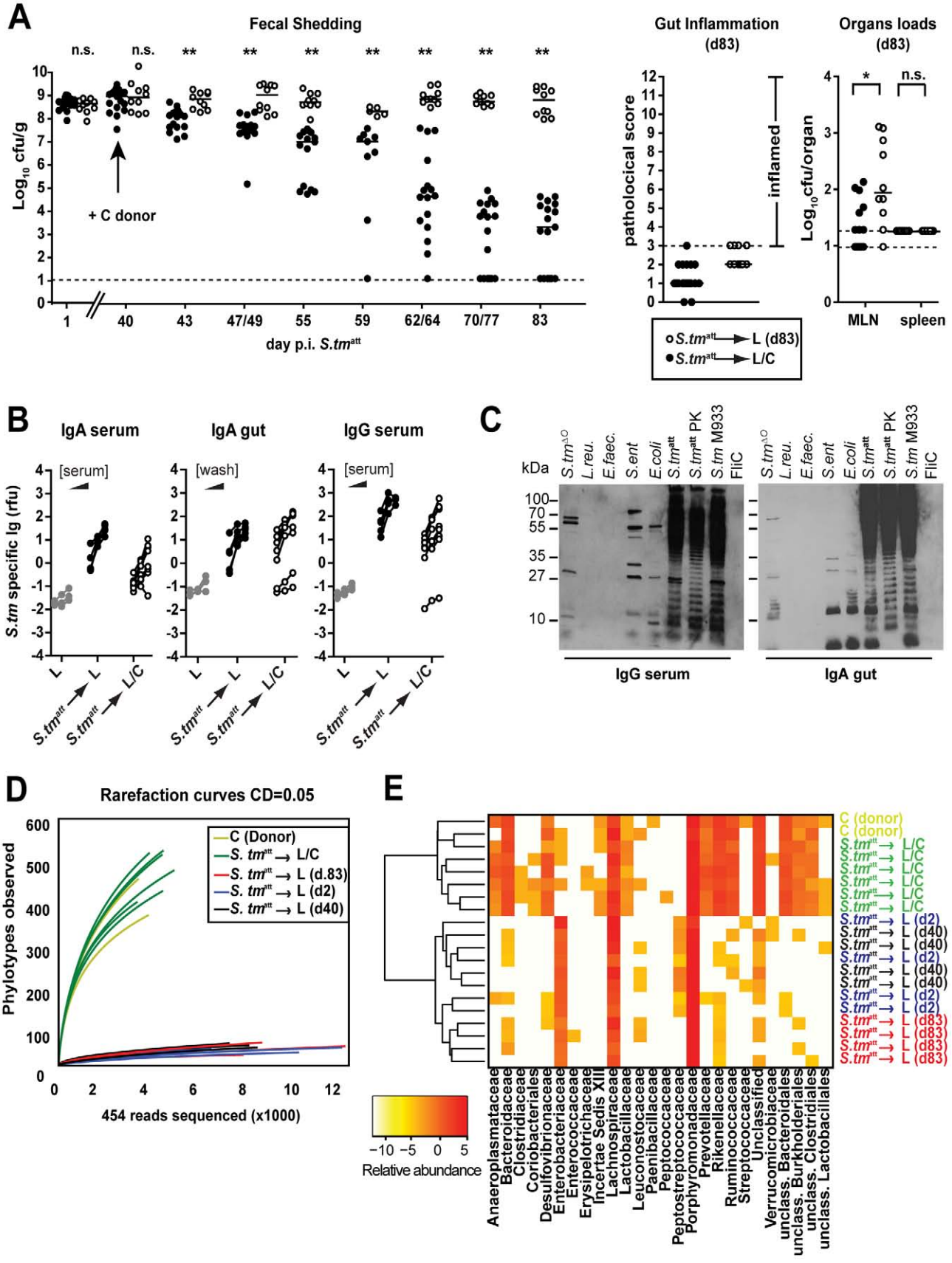


Figure 7. Transfer of a complex microbiota curbs *S. tm*^{att} shedding by L-mice. A. Exposure to conventional gut microbiota curbs pathogen shedding by 'asymptomatic excretors'. L-mice were immunized with *S. tm*^{att}. At day 40 p.i., donor animals with a conventional microbiota (C-mice)

were added to one group (black circles; n = 17; *S. tm*^{att}→L/C). The other group remained under hygienic isolation (open circles; n = 10; *S. tm*^{att}→L). Fecal *S. tm*^{att} shedding was monitored until day 83 p.i. Right panels show gut inflammation and organ loads at day 83 p.i.. **B. and C**. *S. tm*-specific Ig-response (serum IgA and IgG; IgA in gut wash; day 83 p.i.) in *S. tm*^{att}→L and *S. tm*^{att}→L/C mice was determined by bacterial FACS and by immunoblot as in Fig. 2A,B. **D**. A complex microbiota is transferred to L-mice by day 83 p. *S. tm*^{att} immunization. Collectors' curves (CD = 0.05) were created for each mouse from the total number of filtered sequences for representative mice: *S. tm*^{att}→L (d.2), *S. tm*^{att}→L (d.40), *S. tm*^{att}→L (d.83), *S. tm*^{att}→L/C and 2 C-mice (donor). **E**. Phylotypes of mice shown in (**D**) (Clustering distance CD = 0.05) were sorted according to their family taxon (family level; x-axis) and average clustering was performed on Euclidean distances calculated between abundance profiles for each mouse and every time-point sampled. Red color indicates high abundance (Log2), yellow color low abundance.
doi:10.1371/journal.ppat.1001097.g007

Materials and Methods

Animals

Specified pathogen-free (SPF) wild type C57BL/6 mice, $J_H^{-/-}$ [48] and $IgA^{-/-}$ [49], $pIgR^{-/-}$ [50] and $TCR\beta^{-/-}\delta^{-/-}$ mice [51] (7–10 weeks old; all C57BL/6 background) were bred at the Rodent center HCI (RCHCI) under barrier conditions in individually ventilated cages (Ehret). $IgA^{-/-}$, $IgA^{+/-}$ and $IgA^{+/+}$ littermates were generated by crossing $IgA^{-/-}$ with C57BL/6 mice and breeding $IgA^{+/-}\times IgA^{+/-}$ animals. L-mice were

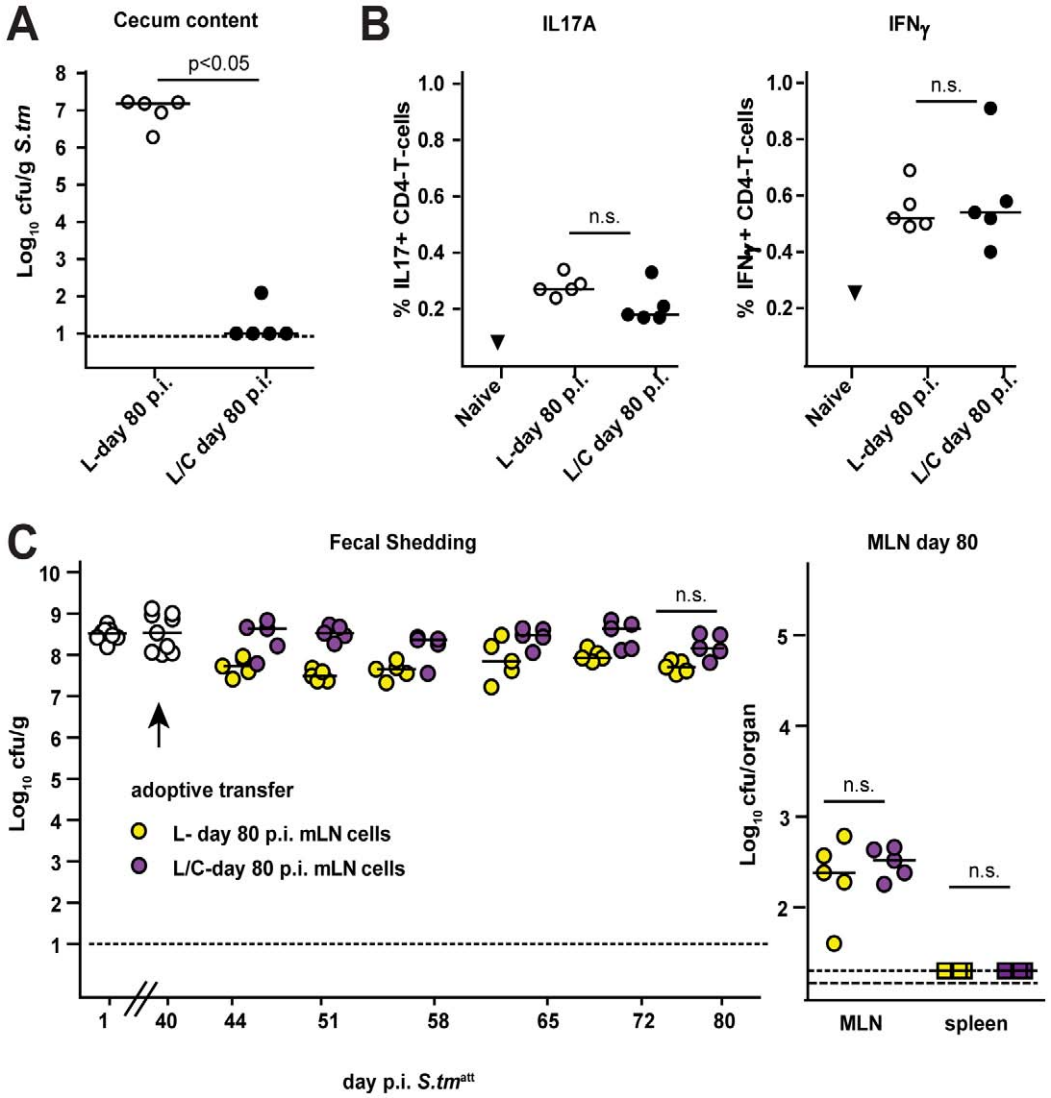


Figure 8. Adoptive transfer of MLN cells isolated form mice that cleared *S. tm*^{att} from the intestine into *S. tm*^{att}→L mice (day 40 p.i.) does not induce *S. tm*^{att} clearance. L-mice were immunized with *S. tm*^{att}. At day 40 p.i., animals with a conventional microbiota (C-mice) were added to one group (black circles; n = 5; *S. tm*^{att}→L/C). The other group remained under hygienic isolation (open circles; n = 5; *S. tm*^{att}→L). **A**. All mice were sacrificed at day 80 p.i. and *S. tm*^{att} levels in the cecal content were defined. **B**. Total MLN cells from the two groups of mice were isolated and analyzed with respect to the expression of intracellular cytokines IL-17A (left) and IFNγ (right) in $CD4^+$ T-cells at day 80 post *S. tm*^{att} infection (% cytokine-expressing $CD4^+$ T-cells). **C**. 3×10^7 MLN cells of 'donor' mice *S. tm*^{att}→L and *S. tm*^{att}→L/C described above were adoptively transferred into another cohort of *S. tm*^{att}→L mice (day 40 p.i.: = 'aceptors'). Fecal *S. tm*^{att} shedding was followed in the 'acceptors' until day 80 post *S. tm*^{att} infection (= day 40 post adoptive transfer, left). *S. tm*^{att} levels in the MLN of 'acceptors' at day 80 post *S. tm*^{att} infection (= day 40 post adoptive transfer, left).
doi:10.1371/journal.ppat.1001097.g008

generated by colonizing germfree C57BL/6 mice with the Altered Schaedler flora (ASF). Mice, housed in a bubble isolator, were inoculated at eight weeks of age by intra-gastric and intra-rectal administration of 10^7–10^8 cfu of ASF bacteria on consecutive days (www.taconic.com/library). Later, L-mice (C57BL/6 background) were maintained under barrier conditions in IVCs with autoclaved chow and autoclaved, acidified water. Mice with complex microbiota were never housed together with these in the same room to prevent contamination with additional commensal bacteria.

Ethics statement

All animal experiments were approved (license 201/2004 and 201/2007 Kantonales Veterinäramt Zürich) and performed according to local guidelines (TschV, Zurich) and the Swiss animal protection law (TschG).

Infection experiments

Salmonella infections were performed in individually ventilated cages at the RCHCI, Zurich, as previously described [52]. In brief, wild type C57BL/6 mice, $J_H^{-/-}$, $IgA^{-/-}$, $pIgR^{-/-}$ and $TCR\beta^{-/-}\delta^{-/-}$ mice were pretreated with 20mg of streptomycin (sm) by gavage. 24h later, the mice were inoculated with 5×10^7 CFU of *S. tm*^{att}, PBS (mock) or as indicated. 'Challenge infections' were performed 40 days later (or as indicated). Mice were treated with ampicillin (20mg; by gavage) and 24h later infected with a dose of 200 CFU of the respective ampicillin-resistant (pM973) challenge strain. Samples of cecal tissue were cryo-embedded, and inflammation was quantified on cryosections (5 µm, cross-sectional) stained with hematoxylin and eosin (H&E). Pathogen-colonization was assessed as described, below.

Histology

H&E-stained cecum cryosections were scored as described, evaluating submucosal edema, PMN infiltration, goblet cells and epithelial damage yielding a total score of 0–13 points [53].

Analysis of *Salmonella* loads in cecal content, mesenteric lymph nodes, and spleen

Mesenteric lymph nodes (MLN), spleen and liver were removed aseptically and homogenized in cold PBS (0.5% tergitol, 0.5% BSA). The cecum content was suspended in 500il cold PBS and bacterial loads were determined by plating on MacConkey agar plates (50 ìg ml^{-1} streptomycin) as described [21]. Colonization levels of the challenge strain (carrying pM973 with an antibiotic marker) and immunization strain (*S. tm*^{att}; km^R) were determined by selective plating (100ìg ml^{-1} ampicillin or 30 ìg ml^{-1} kanamycin; levels of challenge strain: amp^R-km^R *Salmonella*). For co-infection experiments shown in Fig. 2C, competitive indices were calculated according to the formula CI = ratio *S. tm*:*S. en*$_{\text{cecal content}}$/ratio *S. tm*:*S. en*$_{\text{inoculum}}$.

Adoptive transfer of MLN cells

MLN were harvested from *S. tm*^{att}→L (total of 5 mice) and *S. tm*^{att}→L/C (total of 5 mice) at day 80 post *S. tm*^{att} infection. Single cell suspensions were prepared using 100µm cell strainers and 40µg/ml DNAse (Roche). *S. tm*^{att}→L mice (at day 40 post *S. tm*^{att} infection) were injected intravenously with 3×10^7 cells (pooled for each of the two groups) in 200µl PBS. Fecal *S. tm*^{att} shedding was monitored for another 40 days.

Intracellular cytokine staining

Single-MLN-cell suspensions were prepared as described above. For intracellular staining of IFN-γ and IL-17A, 1×10^7 nucleated MLN cells were cultured for 3 h in 1 ml of RPMI 1680 supplemented with 10% heat-inactivated FCS and stimulated with PMA (5pg/ml) /ionomycin (500pg/ml). After adding 20 µg/ml brefeldin A, the cells were incubated for another 3h at 37°C. Cells were harvested and washed in ice-cold FACS buffer (PBS, 2% heat-inactivated FCS, 5 mM EDTA, and 0.02% sodium azide). Cells were resuspended in FACS buffer and stained on the surface with fluorescently-labeled antibodies for 30 min on ice. For intracellular staining of IL-17A and IFN-γ, cells were washed once and fixed/permeabilized for 10 min at room temperature using 500 µl of FIX/perm solution (FACSLyse; BD Biosciences; diluted to 2× concentration in distilled water and 0.05% Tween 20). Cells were washed once and stained with directly conjugated Abs against IFN-γ-APC (BD) and IL-17A-PE (Biolegend). Cells were then washed again and resuspended in PBS. Data were collected on a LSRII flow cytometer (BD Biosciences) and analyzed using FlowJo software (Tree Star).

Gut wash

The intestine was flushed with 2 ml of a washing buffer containing PBS, 0.05M EDTA pH8.0 and 66µM PMSF. Intestinal wash was briefly vortexed and centrifuged at 4°C, 30 min, 40.000 rpm (Eppendorf centrifuge). Aliquots of supernatants were stored at −80°C.

Immunofluorescence microscopy

Bacteria harboring pM973 (GFP expression after tissue entry) in the lamina propria and epithelium were enumerated by fluorescence microscopy as described [22] using cryo-sections of PFA-fixed cecal tissue stained with Armenian hamster anti-CD54 (clone 3E2; stains lamina propria) antibody (Becton Dickinson), Cy3-conjugated goat anti–Armenian hamster Ig (Jackson ImmunoResearch Laboratories), DAPI (stains DNA; Sigma-Aldrich), and Alexa647-conjugated phalloidin (stains polymerized actin; Fluoprobes). We evaluated three 20 µm thick sections of the cecum per mouse and plotted for each mouse the average of the three values.

For detecting *S. tm* and *S. en* pM979 in the gut lumen *in situ*, cecal tissues were recovered and treated as described recently [54]. Briefly, the tissues were fixed in paraformaldehyde (4% in PBS, pH 7.4 over night, 4°C), washed with PBS, equilibrated in PBS (20% sucrose, 0.1% NaN_3 over night, 4°C), embedded in O.C.T. (Sakura, Torrance, CA), snap-frozen in liquid nitrogen and stored at −80°C. Cryosections (7ìm) were air-dried for 2 h at room temperature, fixed in 4% paraformaldehyde (5 min), washed and blocked in 10% (w/v) normal goat serum in PBS for 1h. *S. tm* was detected by staining for 1h with a polyclonal rabbit á-*Salmonella*-O-antigen group B serum (factors 1, 4, 5 and 12, Difco; 1:500 in PBS, 10% (w/v) goat serum) and Cy3-conjugated secondary goat-α-rabbit antibody. *S. en* pM979 expresses *gfp* under the control of a constitutive promoter and bacteria were detected in the green channel. F-Actin (epithelial brush border) was visualized by staining with Alexa-647-conjugated phalloidin, as indicated (Molecular Probes). Sections were mounted with Vectashield hard set (Vector laboratories) and sealed with nail polish. Images were recorded with a microscope (Axiovert 200; Carl Zeiss, Inc.), an Ultraview confocal head (PerkinElmer), and a krypton argon laser (643-RYB-A01; Melles Griot). Infrared, red, and green fluorescence was recorded confocally, and blue fluorescence was recorded by epifluorescence microscopy.

Immunohistochemistry

Frozen consecutive sections of spleen, liver, cecum, colon and small intestine (7ìm thick) were briefly fixed (10 min) in acetone

and blocked for 30 min with phosphate buffered saline (PBS) containing 0.5% bovine serum albumin (BSA). Sections were then incubated with the primary antibody for 1 h at room temperature. Primary antibodies included: B220/CD45R (Pharmingen 553084; 1:200) , CD4 (clone YTS191; 1:200) and CD8 (clone YTS169; 1:200) for T-cells (kindly provided by Rolf Zinkernagel; 1:50), Ly-6G (Gr-1) for neutrophils (clone RB6-8C5; 1:600), F4/80 for macrophages (Serotec MCAP 497; 1:50), CD11c for dendritic cells (BD Biosciences 553800; 1:100) and IgA (rat-anti-mouse IgA; Pharmingen 556969; clone C10-3; 1:4000). Secondary antibodies and detection chromagens were applied and visualized using standard methods (see also [55]).

Statistical analysis

Statistical analysis was performed using the exact Mann-Whitney U test (Prism 4.0c). A P value of <0.05 (two tailed) was considered to be statistically significant. In mouse experiments, values were set to the minimal detectable value (10 cfu for cecum; 10 CFU for MLNs; 20 CFU for the spleen) for samples harboring "no bacteria." Two figures (Fig. 1A and 4F) were generated using the statistical software package R. To assess the distribution of *Salmonella* loads in mice during the 60 day infection experiments, median and quantiles (corresponding to 0.05, 0.25, 0.75 and 0.95 probabilities) were plotted for each day or group of days. We performed a linear regression on medians and both 0.05 and 0.95 quantiles, weighted by the number of data points sampled for each day.

The OTUs abundance heatmap represents the mouse normalized OTU abundances (log2) clustered by average linkage clustering on Euclidean distances. This was generated using the function 'heatmap.2' from the 'gplots' R library.

Immunoblot analysis

The equivalent of 1 OD_{600} units/ml (where OD_{600} is the optical density at 600nm) of liquid o.n. cultures of *S.* $tm^{\Delta O}$, *Lactobacillus reuteri* RR, *Enterococcus faecalis*, *S.* en^{wt}, *E.coli*, *S.* tm^{wt}, *S.* tm^{wt} proteinase K treated (Gibco/Life Technologies; 0.4 mg/ml; 1h 57°C) or *S. tm* M933 was pelleted by centrifugation at $14,000\times g$ for 2 min, and the supernatant was discarded. Cells were resuspended in Laemmli sample buffer (0.065 M Tris-HCl [pH 6.8], 2% [wt/vol] sodium dodecyl sulfate [SDS], 5% [vol/vol] β-mercaptoethanol, 10% [vol/vol] glycerol, 0.05% [wt/vol] bromophenol blue) and lysed for 5 min at 95°C. Equal amounts of the different strains and purified *S. tm* flagellin FliC were loaded on a 12% SDS-polyacrylamide gel and proteins wer separated by electrophoresis. Immunoblots were stained with mouse serum (diluted 1:200 in PBS) or intestinal lavages (diluted 1:20 in PBS) from naïve or immunized mice, goat-α-mouse-IgA HRP (Southern Biotech), goat-anti-mouse-IgG HRP (Bethyl Laboratories) and developed using an ECL kit (Amersham). The same protocol was used for the analysis of the human patient serum (dilution 1:20 in PBS), where goat-anti-human-IgA-HRP (2050-05, NEB) and goat-anti-human-IgG-HRP (2040-05, NEB) were used as secondary antibodies.

Bacterial FACS

Analysis was performed as described in [30]. 3ml LB cultures were inoculated from single colonies of plated bacteria and cultured overnight at 37°C without shaking. 1ml of culture was gently pelleted for 4min at 7,000 rpm in an Eppendorf minifuge and washed 3× with sterile-filtered PBS (1% BSA, 0.05% sodium azide) before resuspending to yield a final density of 10^7 bacteria per ml. Mouse serum was diluted 1:20 in PBS (1% BSA, 0.05% sodium azide) and heat-inactivated at 60°C for 30min. The serum solution was then spun at 13,000 rpm in an Eppendorf minifuge for 10min to remove any bacteria-sized contaminants and the supernatant was used to perform serial dilutions (1:20, 1:60, 1:180). 25µl serum solution and 25µl bacterial suspension were mixed and incubated at 4°C for 1h. Bacteria were washed twice before resuspending in monoclonal FITC-anti-mouse IgA (559354; BD Pharmingen), PE-anti-mouse total IgG (715-116-151; Jackson Immunoresearch Europe) and APC-anti-mouse IgM (550676; BD Pharmingen). After a further hour of incubation bacteria were washed once with PBS (1% BSA, 0.05% sodium azide) and then resuspended in PBS (2% PFA) for acquisition on a FACSCalibur using FSC and SSC parameters in logarithmic mode. Data were analysed using FlowJo software (Treestar, USA). Analysis of specific IgA in intestinal lavages was achieved using an identical protocol, using a dilution of 1:2, 1:6 and 1:18 of gut wash.

Microarray-Analysis

The cecum tissue was excised (3 biological replicates per group), washed in cold PBS, placed in 300µl RLT-buffer (RNeasy Mini Kit, Qiagen; 1% β-Mercaptoethanol) and snap-frozen in liquid nitrogen. Total RNA was extracted with the Nucleospin RNA II kit (Macherey Nagel, Germany) and prepared for hybridization as recommended by the manufacturer (Applied biosystems, USA). Briefly, 2µg of total RNA and a T7-oligo(dT) primer were used for reverse transcription. The double-stranded cDNA was purified and converted to DIG labeled-cRNA by in vitro transcription using DIG-UTP (Roche, Germany). The cRNA was purified, fragmented and hybridized on ABI Mouse Genome Survey v2.0 microarrays for 16h. The microarray was washed and incubated with anti-DIG antibodies conjugated to alkaline phosphatase and a chemiluminescent substrate. The microarrays were scanned with the Applied Biosystems 1700 chemiluminescent microarray analyzer [56]. Normalization was achieved using the NeONORM method [57]. Significance of $\log_2$ fold changes ($\log_2$Q) were determined based on a double-log normal distribution hypothesis of signal intensities using mixture ANOVA methodology [56]. A change in the gene expression profiles was considered as significant if $p<0.001$. Heat maps were created according to standard methods [56]. Gene Ontology (GO) annotations were analyzed using the Panther Protein Classification System (http://www.pantherdb.org). Microarray data were deposited in the publicly available database: http://mace.ihes.fr with accession number: 2947924142.

Bacterial DNA extraction and 16SrRNA gene specific PCR

Total DNA was extracted from cecal contents using a QIAmp DNA stool mini kit (Qiagen). Bacterial lysis was enhanced using 0.1mm glass beads in buffer ASF and a Tissuelyzer device (5 minutes, 30Hz; Qiagen). V5-V6 regions of bacterial 16S rRNA were amplified using primers B-V5 (5′ GCCTTGCCAGC CCGCTCAG ATT AGA TAC CCY GGT AGT CC 3′) and A-V6-TAGC (5′GCCTCCCTCGCGCCATCAG [TAGC] AC-GAGCTGACGACARCCATG 3′). The brackets contain one of the 20 different 4-mer tag identifiers [TAGC, TCGA, TCGC, TAGA, TGCA, ATCG, AGCT, AGCG, ATCT, ACGT, GATC, GCTA, GCTC, GATA, GTCA, CAGT, CTGA, CAGA, CTGT, CGTA]. Cycling condition were as follows: 95°C, 10min; 22 cycles of (94°C, 30s; 57°C, 30s; 72°C, 30s); 72°C, 8min; 4°C, ∞; Reaction conditions (50µl) were as follows: 50ng template DNA; 50 mM KCl, 10 mM Tris-HCl pH 8.3, 1.5 mM Mg^{2+}, 0.2mM dNTPs; 40pmol of each primer, 5U of Taq DNA polymerase (Mastertaq; Eppendorf).

PCR products of different reactions were pooled, ethanol-precipitated and fragments of ~300bp were purified by gel

electrophoresis, excised and recovered using a gel-extraction kit (Machery-Nagel). Amplicon sequencing of the PCR products was performed using a 454 FLX instrument (70×70 Picotitre plate) according to the protocol recommended by the supplier (www.454.com). PCR to detect ASF bacteria in the feces was done as described in [42].

Quality filtering and reads sorting

We applied quality control to 454 reads in order to avoid artificial inflation of ecosystem diversity estimates [58]. Reads containing the consensus sequence ('ACGAGCTGACGACA[AG]CCATG') of the V6 reverse primer were filtered with respect to their length (200nt≤length≤300nt). Quality filtering was then applied to include only sequences containing one of the exact 4nt tag sequences and displaying at maximum one ambiguous nucleotide 'N'. The latter criterion has been reported as a good indicator of sequence quality for a single read [41]. We identified 6,754 reads with an incorrect primer sequence, 1,155 reads shorter than 200nt, 8 reads longer than 300nt and 119 reads containing more than one 'N'. After filtering, 140,237 reads remained (out of an initial total of 149,786 raw reads) and were processed as described below for OTU definition and chimera filtering. To estimate the reliability of sample discrimination using our primer-tagging approach, we assessed the number of reads observed to have an illegitimate 4-mer tag (i.e., different from our set of 20 tags). The sequencing plate produced a total of 141,784 quality-filtered reads from which 1,547 contained an incorrect tag (1.09%). Given that 256 distinct 4-mer tags are possible and that we used only 20 of these, the majority of sequencing or primer errors in this region are detectable. Correcting for the small fraction of undetectable errors (20/256) and division by four yields an error rate of 0.296% per single nucleotide - at the position of the tag in the primer (this includes errors during primer synthesis as well as sequencing). Since most errors are actually visible as errors, the rate of unintentional 'miscall' of sample identity is 0.092%.

Definition of OTUs

To reduce computational time and complexity, we built OTUs using the complete filtered dataset covering all non-redundant reads from the 20 samples. Exactly identical sequences were represented by one representative only; after OTU computation, redundant sequences were taken into account for OTU abundance analysis. For subsequent taxonomy classification, we included additional quality-filtered 16S rRNA reference sequences, selected from the Greengenes database (http://greengenes.lbl.gov/Download/Sequence_Data/Greengenes_format/greengenes16SrRNAgenes.txt.gz, release 01-28-2009 [59]). This reference database is based on full-length non-chimerical sequences with a minimum length of 1100nt (in order to fully cover the V6 region of all entries). No archaeal sequences were included in the analysis.

The alignment of non-redundant reads from all mice with the reference database was performed using the secondary-structure aware Infernal aligner (http://infernal.janelia.org/, release 1.0, [60]) and based on the 16S rRNA bacterial covariance model of the RDP database (http://rdp.cme.msu.edu/; [61]). Before defining OTUs, we first removed reference sequences for which the alignment was not successful (Infernal bit-score<0). The alignment was then processed to include an equivalent amount of information from every read. To do so, we identified the consensus reverse primer sequence of the V6 region within the aligned sequence of *Escherichia coli* K12, as a reference. The full alignment was then trimmed from the start position (defined by the *E. coli* V6 reverse primer) and ended after 200nt. This also ensured a further limitation of the effect of pyrosequencing errors by trimming the 3′ end of each read, a region which is more sequencing-error prone (the trimmed and aligned reads length ranged from 152 to 231nt) [58]. Using this alignment, OTUs were built by hierarchical cluster analysis at various distances (0.01, 0.03, 0.05 and 0.10) using the 'complete linkage clustering' tool of the RDP pyrosequencing pipeline http://pyro.cme.msu.edu/ ; [61]).

Taxonomy assignment

In a first step, taxonomy was inferred for all reads using the stand-alone version of the RDP classifier (http://sourceforge.net/projects/rdp-classifier, revision 2.0, [62]). Taxon-level predictions were considered reliable when supported by a minimum bootstrap value of 80%. In order to predict taxonomy for each OTU, we either used any reference sequences present within a cluster, or the taxonomy of the reads present in the cluster, as predicted by the RDP classifier. To increase the resolution of the prediction, we privileged any reference sequences over the reads. For each OTU, taxonomy was inferred by a simple majority vote: if more than half of the reference sequences (or reads) present within a cluster agreed on a taxon, the OTU was annotated according to this taxon. In case of conflicts, we assigned a consensus taxon to a higher phylogenetic level for which the majority vote condition was met.

Chimera estimation

Deep pyrosequencing on the 454 platform has revealed extensive microbial diversity that was previously undetected with culture-dependent methods [63]. Nevertheless, sequencing data generated from pools of PCR products have to be interpreted carefully; limitations and biases of the PCR technique have to be taken into account. This can lead to over-estimations of microbial diversity as has been recently reported [58,64]. Moreover, during amplification, chimerical sequences can be generated.

On such short sequences, recombination points (recombination can occur from an incompletely extended primer or by template-switching; [65]) are extremely difficult to detect. Recently, a new tool to filter noise and remove chimera in 454 pyrosequencing data has been published [64]. There, the authors suggest that because of sequencing errors, diversity estimates may be at least an order of magnitude too high. To our best knowledge, at the time of our analysis, there were no available tools to detect chimera within libraries of short 454 reads. Therefore, in order to detect chimeras we decided to compare taxonomies assigned to N-terminal and C-terminal read fragments using BLASTn. In order to ensure a reasonable alignment length and a relatively high identity to the matching reference sequences, we only analyzed reads for which both fragments had a minimum identity of 95% and a minimum bit-score of 150 (these cutoffs were selected heuristically). A given read was deemed chimeric when the taxonomies of the best hits of each half were clearly not congruent (i.e., differing at the phylum level). Our simple chimera detection method resulted in a slightly higher rate of detected chimera compared to the method of Quince *et al.*, 2009 (~4.5% compare to ~3% in their example), suggesting that our approach is at least of comparable stringency [64].

Supporting Information

Figure S1 'Bacterial FACS' assay for detection of a *Salmonella*-surface-specific immunoglobulins (Ig). **A.** Experimental design for detection of bacteria specific antibodies via FACS analysis. Antibodies directed against the surface of *Salmonella typhimurium* in murine serum or intestinal lavage were detected by bacterial FACS (Materials and Methods for details) as described previously [30]. Overnight cultures of *S. tm*^{att} (approx. 10^6 cfu) were first incubated with decreasing dilutions (1:180, 1:60, 1:20) of serum

from a naïve (upper row) or a mouse at day 21 p.i. with *S. tm*^{att} (lower row). Bacteria-bound IgG was then detected using an anti-mouse-IgG-PE antibody (or α-mouse-IgA-FITC, not shown). **Left panel:** Bacterial gate determined in FSC/SSC (forward-/sideward scatter). **Other panels:** Dot plot (FSC/FL2) showing IgG-PE^{+} bacteria. From these data, we calculated the *Salmonella*-specific Ig (relative fluorescence units) (Materials and Methods; Supplemental Fig1C and Fig.2C, Fig.6B): *S. tm*-specific Ig = (Mean fluorescence intensity of Ig^{+} bacteria§) * (% of positively stained bacteria of all bacteria*). The percentage of positively stained bacteria of all bacteria at the respective dilution is shown in each FACS plot. The mean fluorescence intensity of the Ig^{+} bacteria is shown below each FACS plot. **B.** Antibodies specifically detect *S. tm* but not *E. coli*. *S. tm*^{att} or *E. coli* were incubated with increasing dilutions (1:2; 1:6; 1:18) of an intestinal lavage obtained from a mouse at day 21 p.i. with *S. tm*^{att}. Bacteria-bound IgA was detected by anti-mouse-IgA-FITC. **Upper panel:** Dot plot (FSC/FL1) showing IgA-FITC^{+} *S. tm*^{att}. **Lower panel:** Dot plot (FSC/FL1) showing IgA-FITC^{+} *E.coli*. **C.** Plotting *Salmonella*-specific antibodies. *S*pecific Ig (rfu) against *S. tm*^{att} (*S. tm*^{att} coated; experiment) or *E. coli* (*E. coli* coated; neg. control) for decreasing dilutions (indicated as black slope) of serum (1:180, 1:60, 1:20) or gut wash (1:18, 1:6, 1:2) at day 21 post *S. tm*^{att} immunization were calculated as described in Supplemental Fig.1A and plotted for indicated mice.
Found at: doi:10.1371/journal.ppat.1001097.s001 (0.20 MB TIF)

Figure S2 Immunohistological analysis of *S. tm*^{att}-immunized mice is in line with an adaptive mucosal immune response. **A**. Immunohistological analysis of naïve C57BL/6 mice (conventional SPF gut flora; C-mice) and of mice at day 40 p.i. with *S. tm*^{att}. Quantitative data of Ly6G^{+}, IgA^{+}, CD4^{+} and CD8^{+} cells in cecal tissue of naïve C57BL/6 and day 40 *S. tm*^{att}-immunized mice were obtained by counting 15 randomly selected 40× high power fields (hpf) from 3 mice per group. Y-axis: average cell number per 40× hpf. **B**. Immunohistochemical stainings for Ly6G, IgA, CD4 and CD8 markers were prepared as indicated in Materials and Methods. Scale bar = 50μm.
Found at: doi:10.1371/journal.ppat.1001097.s002 (6.86 MB TIF)

Figure S3 *S. tm*^{att} immunized mice mount an O-antigen specific IgA response. Serum from the same naïve and *S. tm*^{att} infected mice (day 40 p.i.) as shown in Fig. 2D was analyzed by immunoblot against different bacterial lysates (*S. tm*$^{\Delta O}$; *L. reuteri*; *E. faecalis*; *S. en*^{wt}; *E. coli*; *S. tm*^{att}; *S. tm*^{att} digested with proteinase K; *S. tm* M933 [no flagella, no functional TTSS]; flagellin FliC). IgA was detected with a goat-anti-mouse-IgA-HRP secondary antibody. The experiment is representative for 6 different animals.
Found at: doi:10.1371/journal.ppat.1001097.s003 (0.68 MB TIF)

Figure S4 Serum of a *S. tm* infected human patient ('asymptomatic excretor') shows a *S. tm*-specific serum Ig-response. The human patient had *S. typhimurium*-positive stool cultures for at least two months. The specificity of the Ig-response in the serum was tested by immunoblot against different bacterial lysates (*S. tm*$^{\Delta O}$; *L. reuteri*; *E. faecalis*; *S. en*^{wt}; *E. coli*; *S. tm*^{att}; *S. tm*^{att} digested with proteinase K; *S. tm* M933 [no flagella, no functional TTSS]; flagellin FliC). Bound human Igs were detected using anti-human-IgA-HRP and anti-human-IgG-HRP secondary antibodies. The patient serum revealed *S. tm*- (but not *S. en*)-O-antigen-specific IgA- and IgG-responses. We speculate that the *E. coli*-O-antigen-specific antibodies might be attributable to a previous exposure to pathogenic *E. coli* spp.. However, this has not been analyzed.
Found at: doi:10.1371/journal.ppat.1001097.s004 (1.00 MB TIF)

Figure S5 An acute inflammatory response in the gut might be required for the induction of *S. tm*-specific mucosal IgA. Non-sm-treated *S. tm*^{att} immunized, sm-treated *S. tm*^{avir}-immunized as well as *S. tm*^{att} i.v. immunized mice do not mount a *Salmonella*-specific adaptive IgA response and are not protected against colitis upon challenge with *S. tm*^{wt}. **A**. The first group of C57BL/6 mice (n = 5; black symbols) was pretreated with sm and immunized with *S. tm*^{avir} (5×10^{7} cfu by gavage). The second group of C57BL/6 mice (n = 5; blue symbols) was <u>not</u> pretreated with sm and immunized with *S. tm*^{att} (5×10^{7} cfu by gavage). The third group of C57BL/6 mice (n = 5; green symbols) was <u>not</u> pretreated with sm and immunized with *S. tm*^{att} (5×10^{5} cfu i.v.). At day 40 p.i. mice were treated with ampicillin and orally challenged with *S. tm*^{wt} (200 cfu by gavage). Mice were sacrificed at day 2 post challenge and *Salmonella* loads in the cecal content (left panel) and the MLN (middle panel) were determined. Cecal pathology was evaluated (right panel). **B**. *Salmonella*-specific sIgA response. Ig-specific antibody responses against different bacterial lysates (*S. tm*$^{\Delta O}$; *L. reuteri*; *E. faecalis*; *S. en*^{wt}; *E. coli*; *S. tm*^{att}; *S. tm*^{att} digested with proteinase K; *S. tm* M933 [no flagella, no functional TTSS]; flagellin FliC) were tested by immunoblot analysis. Immunoblots were incubated with serum or gut wash of sm-treated *S. tm*^{avir} immunized mice, non-sm-treated *S. tm*^{att}-immunized or *S. tm*^{att} i.v. immunized mice that were orally challenged with *S. tm*^{wt} at day 40 p.i.. Specific antibodies were detected with an anti-mouse-IgA-HRP conjugate.
Found at: doi:10.1371/journal.ppat.1001097.s005 (1.27 MB TIF)

Figure S6 Antibody responses of *S. tm*^{att} immunized $J_H^{-/-}$ IgA$^{-/-}$, pIgR$^{-/-}$ and TCRβ$^{-/-}$δ$^{-/-}$ mice. The specific Ig-response of the mice shown in Table 1 (day 40 post immunization with *S. tm*^{att}) was analyzed by Western blot using different bacterial lysates (*S. tm*$^{\Delta O}$; *L. reuteri*; *E. faecalis*; *S. en*^{wt}; *E. coli*; *S. tm*^{att}; *S. tm*^{att} digested with proteinase K; *S. tm* M933 [no flagella, no functional TTSS]; flagellin FliC). Serum or gut wash of d 40 *S. tm*^{att}-immunized knockout mice was tested and specific antibodies were detected with anti-mouse-IgA-HRP or anti-mouse-IgG-HRP conjugates. Panels show specificity of Ig in serum and gut wash of the indicated knock-out mice. Slight amounts of *S. tm* specific sIgA were detected in the gut wash of pIgR$^{-/-}$ mice. We speculate that this is attributable to the 10-fold increased serum IgA levels and consequent leakage in to the gut lumen as described before [18,66] and our own data (not shown).
Found at: doi:10.1371/journal.ppat.1001097.s006 (3.32 MB TIF)

Figure S7 Serovar specificity of the anti-LPS antibody response. *S. tm*^{att} and *S. en*^{att} immunized C57BL/6 mice mount a serovar-specific serum IgA response by day 40 p.i.. Sera of *Salmonella*-or mock-immunized mice were analyzed by immunoblot using anti-mouse-IgA-HRP antibody against lysates of *S. tm*^{att} and *S.en*, respectively. **Left panel:** Serum of a *S. tm*^{att}-immunized C57BL/6 mouse. **Middle panel:** Serum of a *S. en*^{att}-immunized C57BL/6 mouse. **Right panel:** Serum of a mock immunized C57BL/6 mouse.
Found at: doi:10.1371/journal.ppat.1001097.s007 (0.32 MB TIF)

Figure S8 L-mice mount a LPS-O-antigen-specific sIgA response by day 40 post *S. tm*^{att} infection. The specific Ig-response of the mice shown in Fig. 4A (day 40 post immunization with *S. tm*^{att}) was analyzed by Western blot using different bacterial lysates (*S. tm*$^{\Delta O}$; *L. reuteri*; *E. faecalis*; *S. en*^{wt}; *E. coli*; *S. tm*^{att}; *S. tm*^{att} digested with proteinase K; *S. tm* M933 [no flagella, no functional TTSS]; flagellin FliC). Serum or gut wash was tested and specific antibodies were detected with anti-mouse-IgA-HRP or anti-mouse-IgG-HRP conjugates.
Found at: doi:10.1371/journal.ppat.1001097.s008 (0.58 MB TIF)

Figure S9 Protein association network of genes significantly upregulated in the cecal mucosa of *S. tm*^{att}→L mice. Gene expression profiles of the cecal mucosa of naïve L and *S. tm*^{att}→L

mice (day 40) were determined using mouse gene expression microarrays (see Materials and Methods; Supplemental Table 3). Genes significantly up-regulated in the cecal mucosa of *S. tm*^{att}→L mice at day 40 p.i. (compared to naïve L-mice) were determined (significance of $\log_2$ fold changes $p<0.001$) and protein functional interactions visualized using STRING version 8.2 [67]. Colors denote the results of unsupervised clustering of the interaction network, the resulting clusters are indicative of proteins with related biological function and are annotated by GO categories assigned to genes detected as significantly up-regulated. For some gene groups, biological functions were added to ease understanding (i.e. T-cell-mediated immunity, immunity and defense, MHCI, MHCII, B-cell and antibody mediated immunity, cytokines and chemokines). Parameters used in STRING (Active Prediction Methods (connecting lines): Text mining (yellow), Neighborhood (green), Gene Fusion (red), Co-occurrence (blue), Co-expression (black), Experiments (purple), Databases (turquoise) ; confidence score: 0.15; Network clustering (KMeans: 10).
Found at: doi:10.1371/journal.ppat.1001097.s009 (0.42 MB TIF)

Table S1 Bacterial strains and plasmids used in this study.
Found at: doi:10.1371/journal.ppat.1001097.s010 (0.36 MB PDF)

Table S2 Mice used in this study.
Found at: doi:10.1371/journal.ppat.1001097.s011 (0.19 MB PDF)

Table S3 Pathways significantly over-represented among the differentially expressed genes in the cecal mucosa of L-mice at day 40 p.i. with *S. tm*^{att}.
Found at: doi:10.1371/journal.ppat.1001097.s012 (0.47 MB PDF)

Table S4 Quantitative microbiota analysis by 454 amplicon sequencing.
Found at: doi:10.1371/journal.ppat.1001097.s013 (0.39 MB PDF)

Acknowledgments

We are grateful to Roy Curtiss III, Sarkis Mazmanian, Annette Oxenius, Manfred Kopf, Roman Spörri, Markus Aebi and Benjamin Misselwitz for discussions and in depth comments on the manuscript, A. Oxenius for TCR$\beta^{-/-}\delta^{-/-}$ mice, Nicola Harris for IgA$^{-/-}$ mice and to Thomas C. Weber, Susanne Freedrich, Manja Barthel and the RCHCI team as well as Marzanna Kuenzli and Weihong Qi at the Functional Genomics Center Zurich for excellent support.

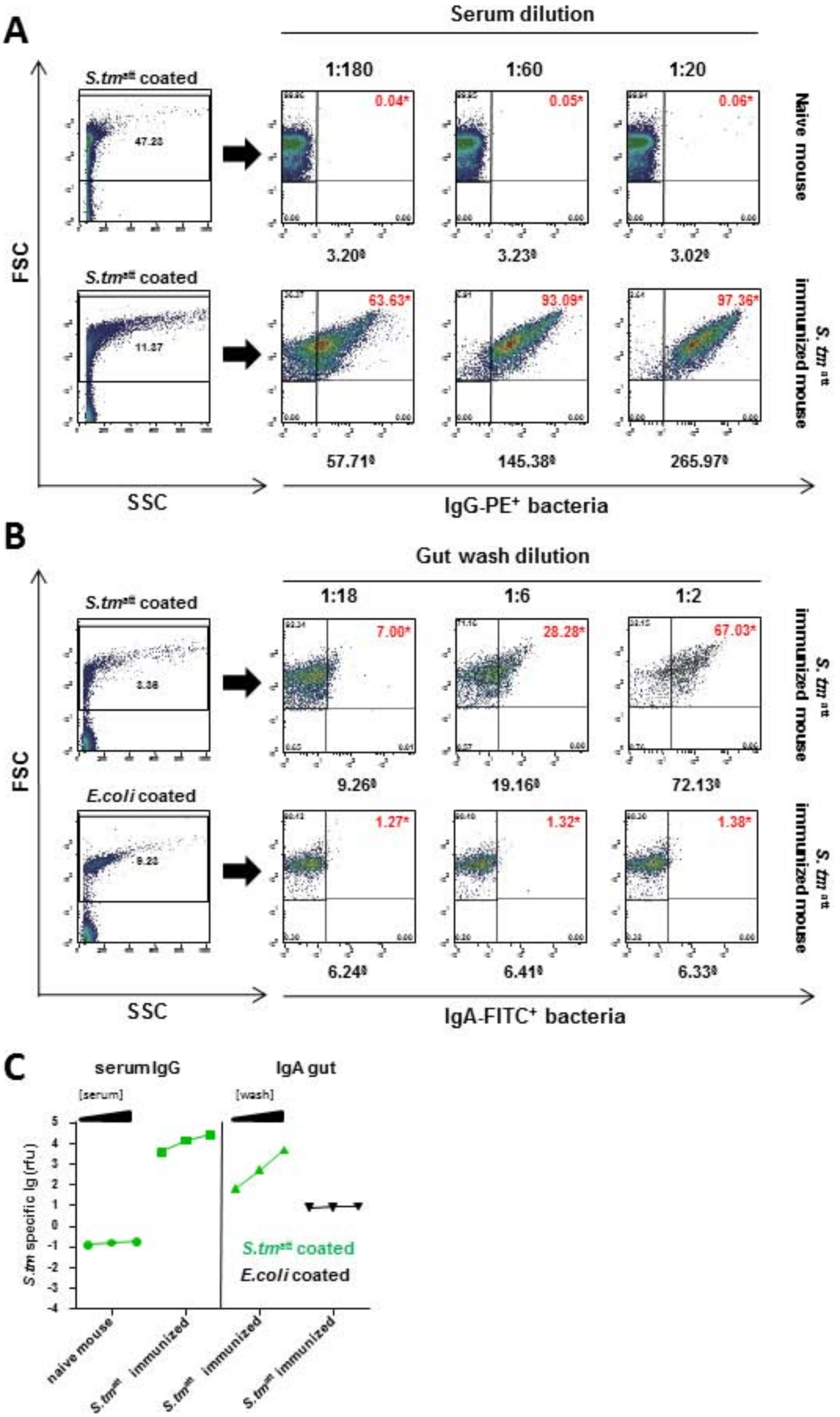
Author Contributions

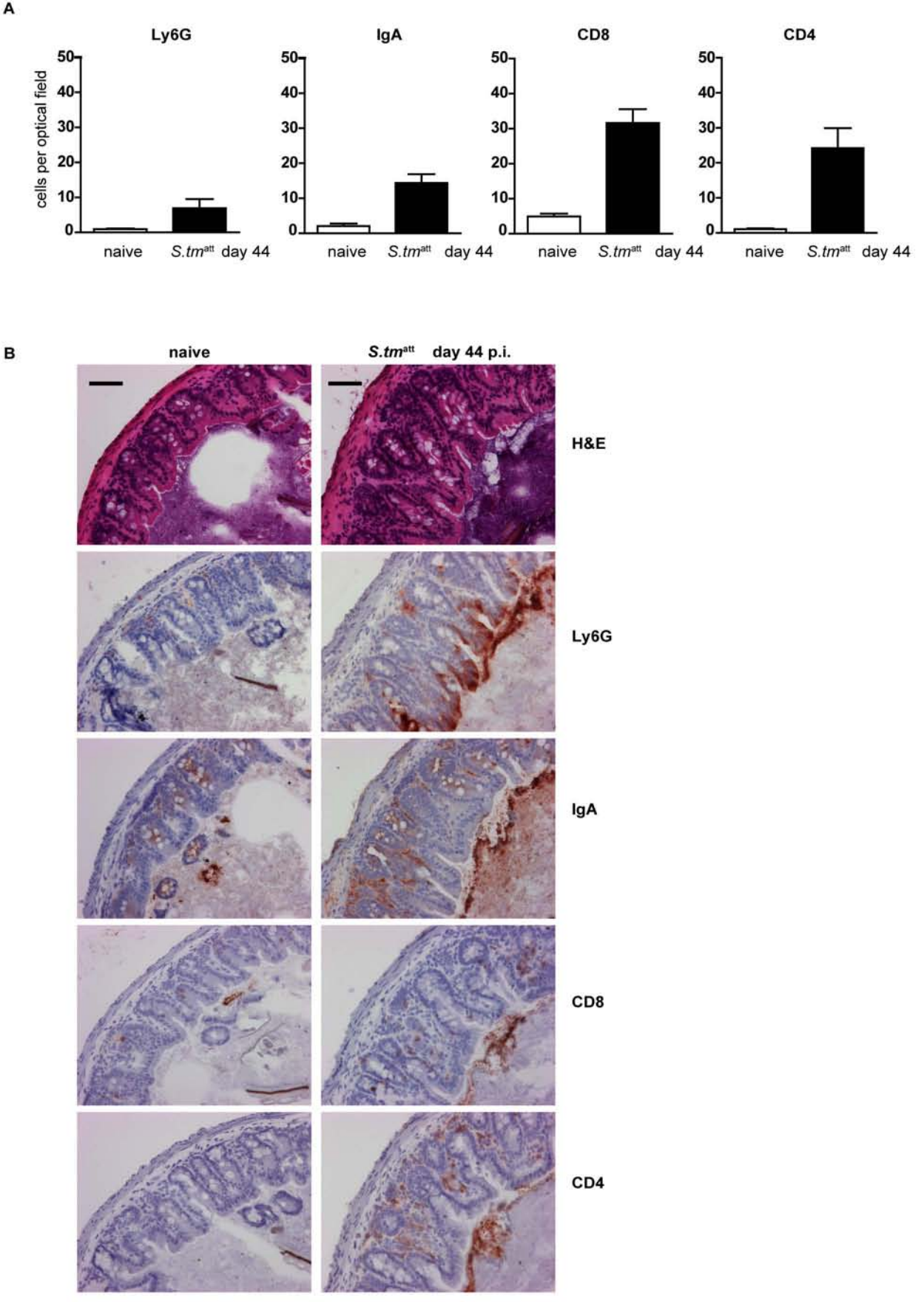
Conceived and designed the experiments: KE BS WDH. Performed the experiments: KE BS. Analyzed the data: KE BS SC ES NT AB LVM JCS AJM MH. Contributed reagents/materials/analysis tools: ES AB JCS AJM RS CvM. Wrote the paper: BS WDH.

References

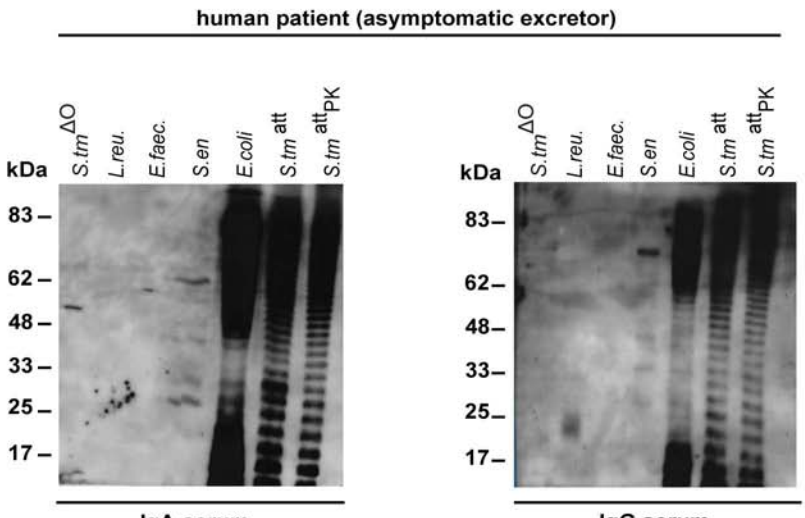
1. Backhed F, Ley RE, Sonnenburg JL, Peterson DA, Gordon JI (2005) Host-bacterial mutualism in the human intestine. Science 307: 1915–1920.
2. Ivanov II, Atarashi K, Manel N, Brodie EL, Shima T, et al. (2009) Induction of intestinal Th17 cells by segmented filamentous bacteria. Cell 139: 485–498.
3. van der Waaij D, Berghuis-de Vries JM, Lekkerkerk L-v (1971) Colonization resistance of the digestive tract in conventional and antibiotic-treated mice. J Hyg (Lond) 69: 405–411.
4. Vollaard EJ, Clasener HA (1994) Colonization resistance. Antimicrob Agents Chemother 38: 409–414.
5. Stecher B, Hardt WD (2008) The role of microbiota in infectious disease. Trends Microbiol 16: 107–114.
6. Barthel M, Hapfelmeier S, Quintanilla-Martinez L, Kremer M, Rohde M, et al. (2003) Pretreatment of mice with streptomycin provides a Salmonella enterica serovar Typhimurium colitis model that allows analysis of both pathogen and host. Infect Immun 71: 2839–2858.
7. Barman M, Unold D, Shifley K, Amir E, Hung K, et al. (2008) Enteric salmonellosis disrupts the microbial ecology of the murine gastrointestinal tract. Infect Immun 76: 907–915.
8. Hohmann EL (2001) Nontyphoidal salmonellosis. Clin Infect Dis 32: 263–269.
9. Dethlefsen L, Huse S, Sogin ML, Relman DA (2008) The Pervasive Effects of an Antibiotic on the Human Gut Microbiota, as Revealed by Deep 16S rRNA Sequencing. PLoS Biol 6: e280.
10. Dore K, Buxton J, Henry B, Pollari F, Middleton D, et al. (2004) Risk factors for Salmonella typhimurium DT104 and non-DT104 infection: a Canadian multi-provincial case-control study. Epidemiol Infect 132: 485–493.
11. Buchwald DS, Blaser MJ (1984) A review of human salmonellosis: II. Duration of excretion following infection with nontyphi Salmonella. Rev Infect Dis 6: 345–356.
12. Balfour AE, Lewis R, Ahmed S (1999) Convalescent excretion of Salmonella enteritidis in infants. J Infect 38: 24–25.
13. Greig JD, Todd EC, Bartleson CA, Michaels BS (2007) Outbreaks where food workers have been implicated in the spread of foodborne disease. Part 1. Description of the problem, methods, and agents involved. J Food Prot 70: 1752–1761.
14. Bader MW, Sanowar S, Daley ME, Schneider AR, Cho U, et al. (2005) Recognition of antimicrobial peptides by a bacterial sensor kinase. Cell 122: 461–472.
15. Gunn JS, Lim KB, Krueger J, Kim K, Guo L, et al. (1998) PmrA-PmrB-regulated genes necessary for 4-aminoarabinose lipid A modification and polymyxin resistance. Mol Microbiol 27: 1171–1182.
16. Brown A, Hormaeche CE (1989) The antibody response to salmonellae in mice and humans studied by immunoblots and ELISA. Microb Pathog 6: 445–454.
17. Mittrucker HW, Raupach B, Kohler A, Kaufmann SH (2000) Cutting edge: role of B lymphocytes in protective immunity against Salmonella typhimurium infection. J Immunol 164: 1648–1652.
18. Uren TK, Wijburg OL, Simmons C, Johansen FE, Brandtzaeg P, et al. (2005) Vaccine-induced protection against gastrointestinal bacterial infections in the absence of secretory antibodies. Eur J Immunol 35: 180–188.
19. Maaser C, Housley MP, Iimura M, Smith JR, Vallance BA, et al. (2004) Clearance of Citrobacter rodentium requires B cells but not secretory immunoglobulin A (IgA) or IgM antibodies. Infect Immun 72: 3315–3324.
20. Stecher B, Chaffron S, Kappeli R, Hapfelmeier S, Freedrich S, et al. (2010) Like will to like: abundances of closely related species can predict susceptibility to intestinal colonization by pathogenic and commensal bacteria. PLoS Pathog 6: e1000711.
21. Stecher B, Robbiani R, Walker AW, Westendorf AM, Barthel M, et al. (2007) Salmonella enterica Serovar Typhimurium Exploits Inflammation to Compete with the Intestinal Microbiota. PLoS Biol 5: e244.
22. Hapfelmeier S, Stecher B, Barthel M, Kremer M, Müller A, et al. (2005) The Salmonella Pathogenicity Island (SPI)-1 and SPI-2 Type III Secretion Systems Allow Salmonella Serovar Typhimurium to trigger Colitis via MyD88-Dependent and MyD88-Independent Mechanisms. J Immunol 174: 1675–1685.
23. Coombes BK, Coburn BA, Potter AA, Gomis S, Mirakhur K, et al. (2005) Analysis of the contribution of Salmonella pathogenicity islands 1 and 2 to enteric disease progression using a novel bovine ileal loop model and a murine model of infectious enterocolitis. Infect Immun 73: 7161–7169.
24. Hapfelmeier S, Hardt WD (2005) A mouse model for S. typhimurium-induced enterocolitis. Trends Microbiol.
25. Curtiss R, 3rd, Kelly SM, Hassan JO (1993) Live oral avirulent Salmonella vaccines. Vet Microbiol 37: 397–405.
26. Simonsen J, Molbak K, Falkenhorst G, Krogfelt KA, Linneberg A, et al. (2009) Estimation of incidences of infectious diseases based on antibody measurements. Stat Med 28: 1882–1895.
27. Angelakopoulos H, Hohmann EL (2000) Pilot study of phoP/phoQ-deleted Salmonella enterica serovar typhimurium expressing Helicobacter pylori urease in adult volunteers. Infect Immun 68: 2135–2141.
28. Kang HY, Srinivasan J, Curtiss R, 3rd (2002) Immune responses to recombinant pneumococcal PspA antigen delivered by live attenuated Salmonella enterica serovar typhimurium vaccine. Infect Immun 70: 1739–1749.
29. Bergman MA, Cummings LA, Barrett SL, Smith KD, Lara JC, et al. (2005) CD4+ T cells and toll-like receptors recognize Salmonella antigens expressed in bacterial surface organelles. Infect Immun 73: 1350–1356.
30. Slack E, Hapfelmeier S, Stecher B, Velykoredko Y, Stoel M, et al. (2009) Innate and adaptive immunity cooperate flexibly to maintain host-microbiota mutualism. Science 325: 617–620.
31. Martinoli C, Chiavelli A, Rescigno M (2007) Entry route of Salmonella typhimurium directs the type of induced immune response. Immunity 27: 975–984.
32. Wijburg OL, Uren TK, Simpfendorfer K, Johansen FE, Brandtzaeg P, et al. (2006) Innate secretory antibodies protect against natural Salmonella typhimurium infection. J Exp Med 203: 21–26.
33. Macpherson AJ, Gatto D, Sainsbury E, Harriman GR, Hengartner H, et al. (2000) A primitive T cell-independent mechanism of intestinal mucosal IgA responses to commensal bacteria. Science 288: 2222–2226.
34. Brandtzaeg P (2009) Mucosal immunity: induction, dissemination, and effector functions. Scand J Immunol 70: 505–515.

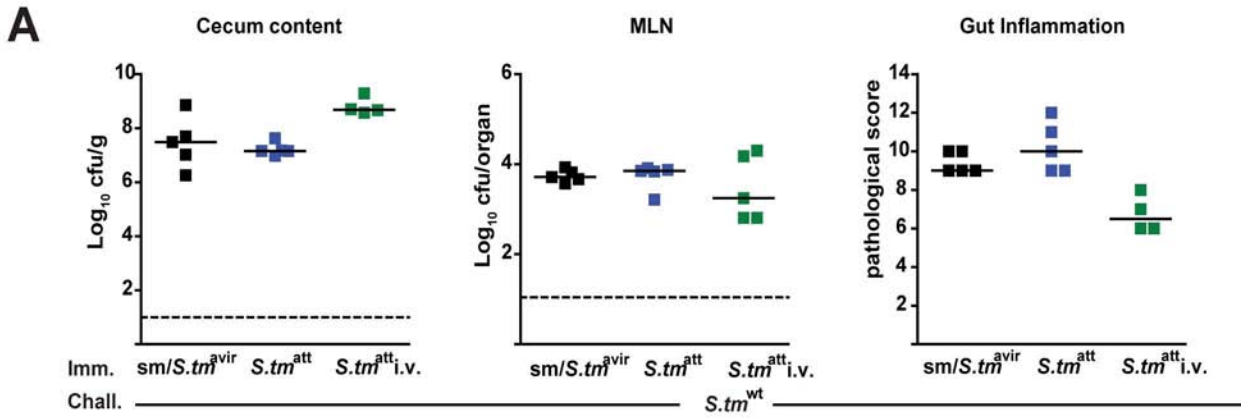
35. Suar M, Periaswamy B, Songhet P, Misselwitz B, Muller A, et al. (2009) Accelerated type III secretion system 2-dependent enteropathogenesis by a Salmonella enterica serovar enteritidis PT4/6 strain. Infect Immun 77: 3569–3577.
36. Ilg K, Endt K, Misselwitz B, Stecher B, Aebi M, et al. (2009) O-antigen-negative Salmonella enterica serovar Typhimurium is attenuated in intestinal colonization but elicits colitis in streptomycin-treated mice. Infect Immun 77: 2568–2575.
37. Turnbaugh PJ, Hamady M, Yatsunenko T, Cantarel BL, Duncan A, et al. (2008) A core gut microbiome in obese and lean twins. Nature.
38. Duerkop BA, Vaishnava S, Hooper LV (2009) Immune responses to the microbiota at the intestinal mucosal surface. Immunity 31: 368–376.
39. Bohnhoff M, Drake BL, Miller CP (1954) Effect of streptomycin on susceptibility of intestinal tract to experimental Salmonella infection. Proc Soc exp Biol, NY 86: 132–137.
40. Turnbaugh PJ, Hamady M, Yatsunenko T, Cantarel BL, Duncan A, et al. (2009) A core gut microbiome in obese and lean twins. Nature 457: 480–484.
41. Huse SM, Dethlefsen L, Huber JA, Welch DM, Relman DA, et al. (2008) Exploring microbial diversity and taxonomy using SSU rRNA hypervariable tag sequencing. PLoS Genet 4: e1000255.
42. Sarma-Rupavtarm RB, Ge Z, Schauer DB, Fox JG, Polz MF (2004) Spatial distribution and stability of the eight microbial species of the altered schaedler flora in the mouse gastrointestinal tract. Appl Environ Microbiol 70: 2791–2800.
43. Ley RE, Hamady M, Lozupone C, Turnbaugh PJ, Ramey RR, et al. (2008) Evolution of mammals and their gut microbes. Science 320: 1647–1651.
44. Nardi RM, Silva ME, Vieira EC, Bambirra EA, Nicoli JR (1989) Intragastric infection of germfree and conventional mice with Salmonella typhimurium. Braz J Med Biol Res 22: 1389–1392.
45. Rawls J (2007) Enteric infection and inflammation alter gut microbial ecology. Cell host and microbe 2: 73–74.
46. Gaboriau-Routhiau V, Rakotobe S, Lecuyer E, Mulder I, Lan A, et al. (2009) The key role of segmented filamentous bacteria in the coordinated maturation of gut helper T cell responses. Immunity 31: 677–689.
47. Mittrucker HW, Kaufmann SH (2000) Immune response to infection with Salmonella typhimurium in mice. J Leukoc Biol 67: 457–463.
48. Chen J, Trounstine M, Alt FW, Young F, Kurahara C, et al. (1993) Immunoglobulin gene rearrangement in B cell deficient mice generated by targeted deletion of the JH locus. Int Immunol 5: 647–656.
49. Harriman GR, Bogue M, Rogers P, Finegold M, Pacheco S, et al. (1999) Targeted deletion of the IgA constant region in mice leads to IgA deficiency with alterations in expression of other Ig isotypes. J Immunol 162: 2521–2529.
50. Uren TK, Johansen FE, Wijburg OL, Koentgen F, Brandtzaeg P, et al. (2003) Role of the polymeric Ig receptor in mucosal B cell homeostasis. J Immunol 170: 2531–2539.
51. Mombaerts P, Mizoguchi E, Ljunggren HG, Iacomini J, Ishikawa H, et al. (1994) Peripheral lymphoid development and function in TCR mutant mice. Int Immunol 6: 1061–1070.
52. Stecher B, Barthel M, Schlumberger MC, Haberli L, Rabsch W, et al. (2008) Motility allows S. Typhimurium to benefit from the mucosal defence. Cell Microbiol 10: 1166–1180.
53. Hapfelmeier S, Muller AJ, Stecher B, Kaiser P, Barthel M, et al. (2008) Microbe sampling by mucosal dendritic cells is a discrete, MyD88-independent step in DeltainvG S. Typhimurium colitis. J Exp Med 205: 437–450.
54. Stecher B, Hapfelmeier S, Muller C, Kremer M, Stallmach T, et al. (2004) Flagella and Chemotaxis Are Required for Efficient Induction of Salmonella enterica Serovar Typhimurium Colitis in Streptomycin-Pretreated Mice. Infect Immun 72: 4138–4150.
55. Mueller C (2002) Tumour necrosis factor in mouse models of chronic intestinal inflammation. Immunology 105: 1–8.
56. Eilebrecht S, Pellay FX, Odenwalder P, Brysbaert G, Benecke BJ, et al. (2008) EBER2 RNA-induced transcriptome changes identify cellular processes likely targeted during Epstein Barr Virus infection. BMC Res Notes 1: 100.
57. Noth S, Brysbaert G, Benecke A (2006) Normalization using weighted negative second order exponential error functions (NeONORM) provides robustness against asymmetries in comparative transcriptome profiles and avoids false calls. Genomics Proteomics Bioinformatics 4: 90–109.
58. Kunin V, Engelbrektson A, Ochman H, Hugenholtz P (2009) Wrinkles in the rare biosphere: pyrosequencing errors lead to artificial inflation of diversity estimates. Environ Microbiol.
59. DeSantis TZ, Hugenholtz P, Larsen N, Rojas M, Brodie EL, et al. (2006) Greengenes, a chimera-checked 16S rRNA gene database and workbench compatible with ARB. Appl Environ Microbiol 72: 5069–5072.
60. Eddy SR (2002) A memory-efficient dynamic programming algorithm for optimal alignment of a sequence to an RNA secondary structure. BMC Bioinformatics 3: 18.
61. Cole JR, Wang Q, Cardenas E, Fish J, Chai B, et al. (2009) The Ribosomal Database Project: improved alignments and new tools for rRNA analysis. Nucleic Acids Res 37: D141–145.
62. Wang Q, Garrity GM, Tiedje JM, Cole JR (2007) Naive Bayesian classifier for rapid assignment of rRNA sequences into the new bacterial taxonomy. Appl Environ Microbiol 73: 5261–5267.
63. Sogin ML, Morrison HG, Huber JA, Welch DM, Huse SM, et al. (2006) Microbial diversity in the deep sea and the underexplored "rare biosphere". Proc Natl Acad Sci U S A 103: 12115–12120.
64. Quince C, Lanzen A, Curtis TP, Davenport RJ, Hall N, et al. (2009) Accurate determination of microbial diversity from 454 pyrosequencing data. Nat Methods 6: 639–641.
65. Kanagawa T (2003) Bias and artifacts in multitemplate polymerase chain reactions (PCR). J Biosci Bioeng 96: 317–323.
66. Johansen FE, Pekna M, Norderhaug IN, Haneberg B, Hietala MA, et al. (1999) Absence of epithelial immunoglobulin A transport, with increased mucosal leakiness, in polymeric immunoglobulin receptor/secretory component-deficient mice. J Exp Med 190: 915–922.
67. Jensen LJ, Kuhn M, Stark M, Chaffron S, Creevey C, et al. (2009) STRING 8–a global view on proteins and their functional interactions in 630 organisms. Nucleic Acids Res 37: D412–416.

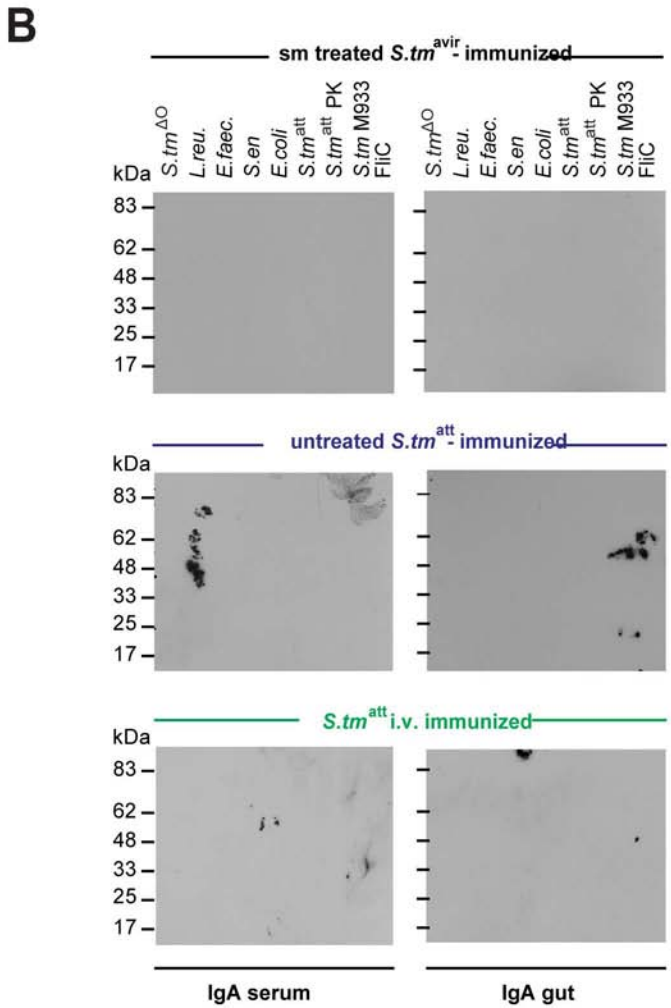

A
Serum dilution
1:180
1:60
1:20
S.tm^stt coated
47.23
0.04*
0.05*
0.06*
Naive mouse
3.20§
3.23§
3.02§
S.tm^stt coated
11.27
63.63*
93.09*
97.36*
S. tm stt immunized mouse
57.71§
145.38§
265.97§
FSC
SSC
IgG-PE+ bacteria
B
Gut wash dilution
1:18
1:6
1:2
S.tm^stt coated
7.00*
28.28*
67.03*
S. tm stt immunized mouse
9.26§
19.16§
72.13§
E.coli coated
1.27*
1.32*
1.38*
S. tm stt immunized mouse
6.24§
6.41§
6.33§
FSC
SSC
IgA-FITC+ bacteria
C
serum IgG
IgA gut
[serum]
[wash]
S.tm specific Ig (rfu)
S.tm^stt coated
E.coli coated
naive mouse
S.tm^stt immunized
S.tm^stt immunized
S.tm^stt immunized


A
Ly6G
IgA
CD8
CD4
cells per optical field
50
40
30
20
10
0
naive
S.tm^att day 44
B
naive
S.tm^att day 44 p.i.
H&E
Ly6G
IgA
CD8
CD4

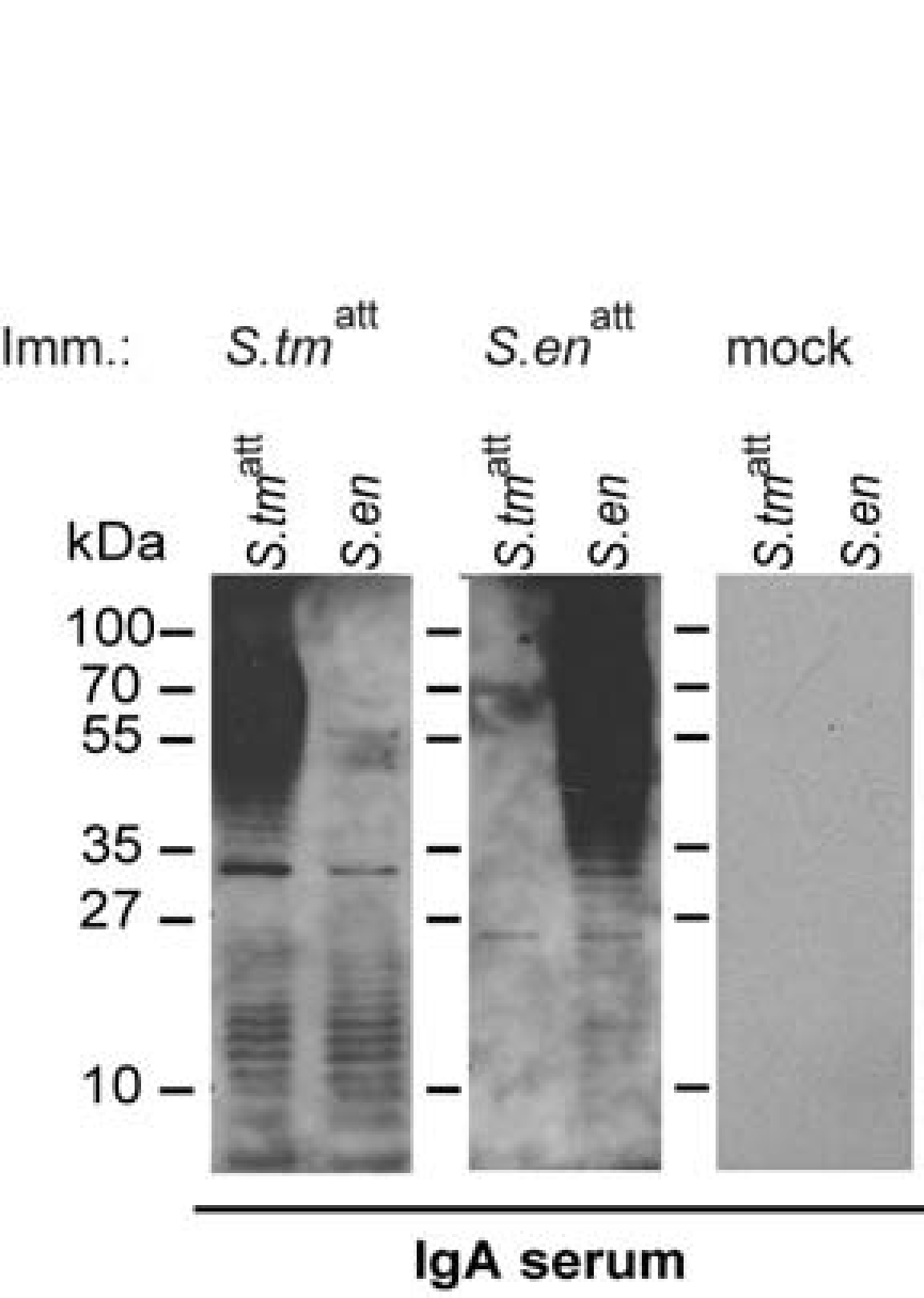
naive
S.tm att - immunized
S.tmΔO
L.reu.
E.faec.
S.en
E.coli
S.tmatt
S.tmattPK
S.tm M933
FliC
kDa
83
62
48
33
25
17
IgA serum

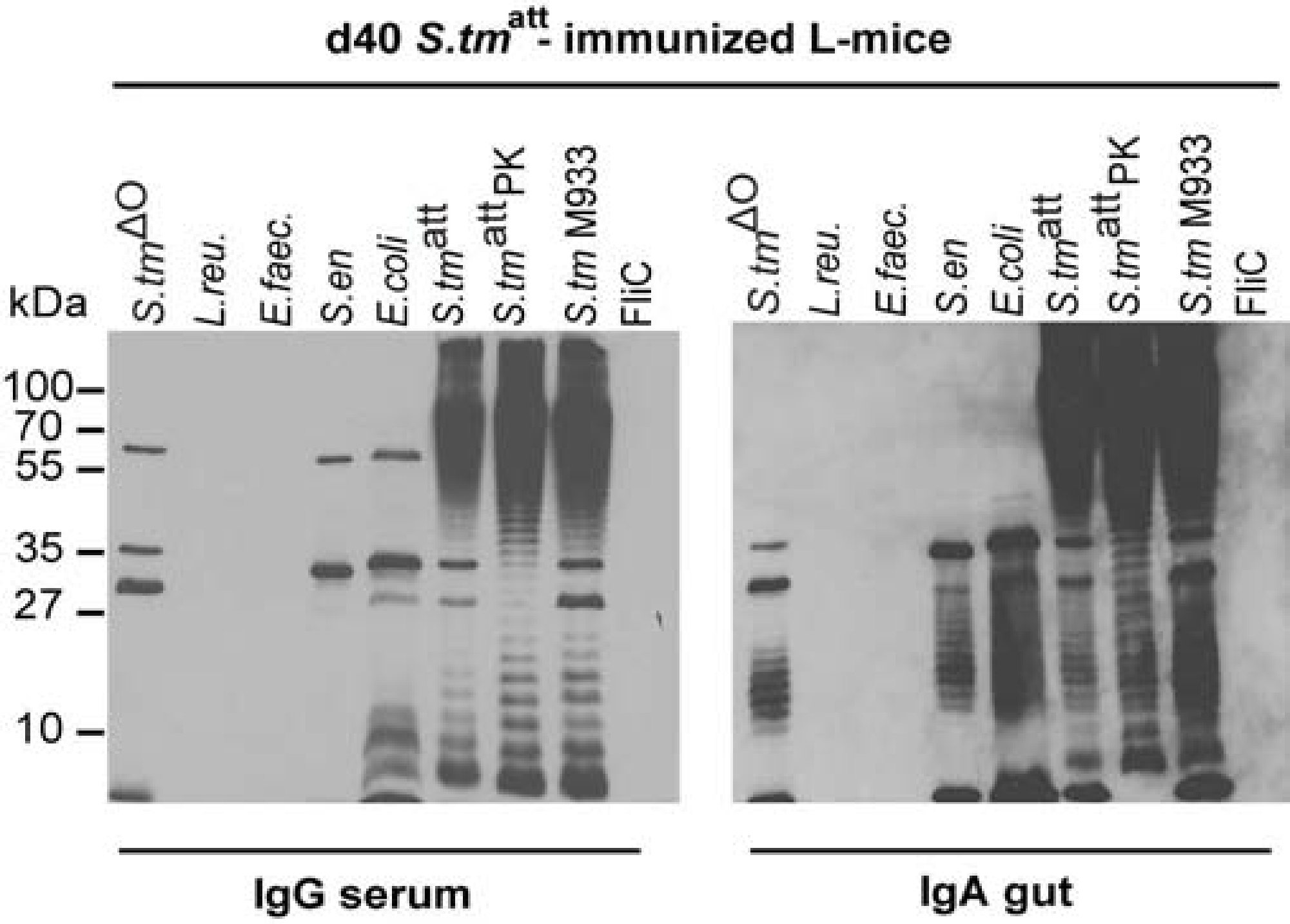

human patient (asymptomatic excretor)
kDa
S.tm ΔO
L.reu.
E.faec.
S.en
E.coli
S.tm att
S.tm attPK
83
62
48
33
25
17
IgA serum
kDa
S.tm ΔO
L.reu.
E.faec.
S.en
E.coli
S.tm att
S.tm attPK
83
62
48
33
25
17
IgG serum

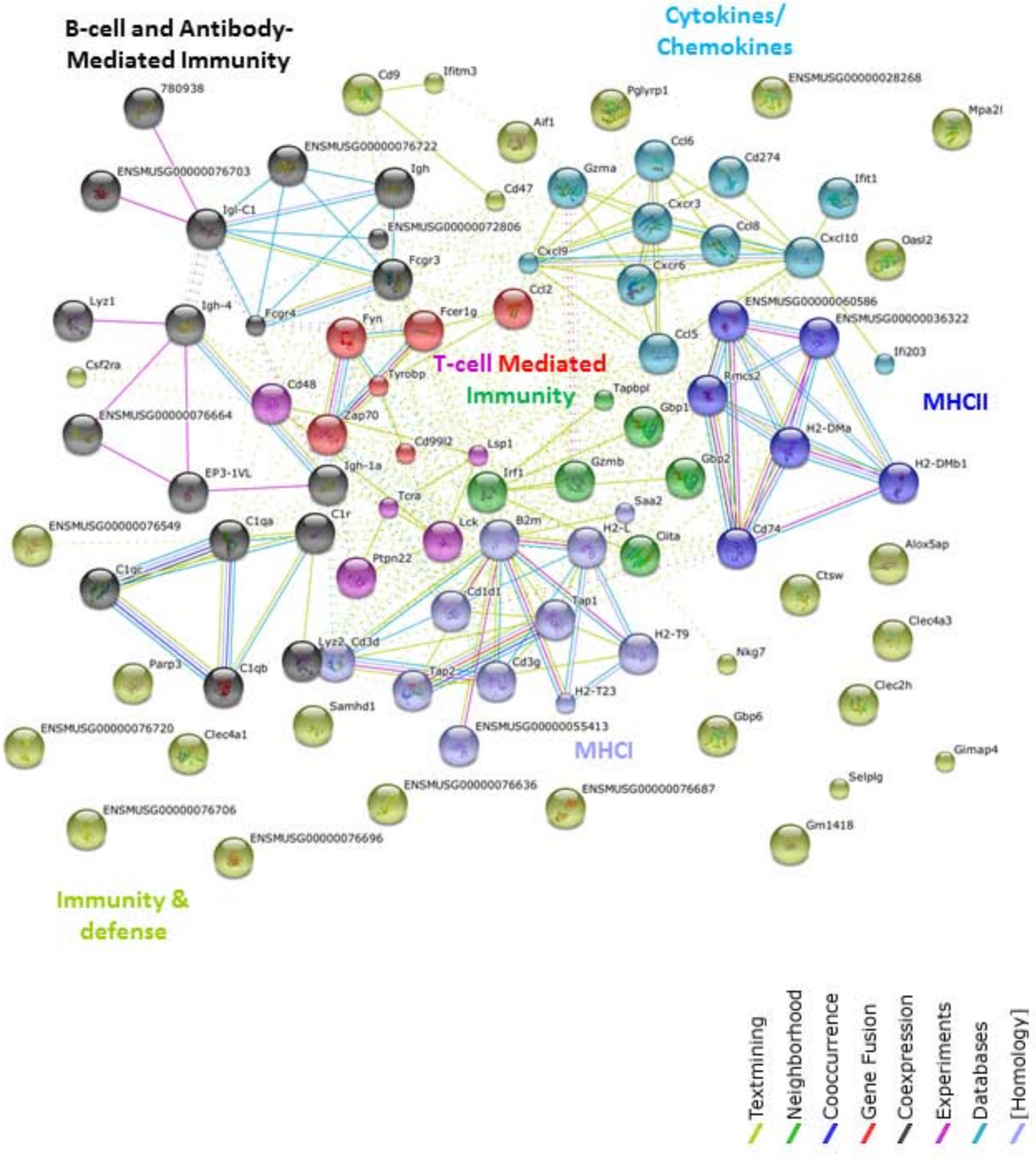

A
Cecum content
MLN
Gut Inflammation
Log10 cfu/g
Log10 cfu/organ
pathological score
Imm.
sm/S.tm^avir
S.tm^att
S.tm^att i.v.
Chall.
S.tm^wt


B
sm treated S.tm^avir - immunized
untreated S.tm^att - immunized
S.tm^att i.v. immunized
S.tmΔO
L.reu.
E.faec.
S.en
E.coli
S.tm^att
S.tm^att PK
S.tm M933 FliC
kDa
83
62
48
33
25
17
IgA serum
IgA gut

S.tm^att- immunized
IgA-/-
pIgR-/-
TCR ß-/-δ-/-
JH-/-
kDa
83
62
48
33
25
17
S.tmΔO
L.reu.
E.faec.
S.en
E.coli
S.tmatt
S.tmatt PK
S.tm M933
FliC
IgA serum
IgG serum
IgA gut


Imm.:
S.tm att
S.en att
mock
kDa
S.tm att
S.en
S.tm att
S.en
S.tm att
S.en
100
70
55
35
27
10
IgA serum


d40 S.tm^att - immunized L-mice
kDa
100
70
55
35
27
10
S.tm^ΔO
L.reu.
E.faec.
S.en
E.coli
S.tm^att
S.tm^attPK
S.tm M933
FliC
S.tm^ΔO
L.reu.
E.faec.
S.en
E.coli
S.tm^att
S.tm^attPK
S.tm M933
FliC
IgG serum
IgA gut


B-cell and Antibody-Mediated Immunity
Cytokines/ Chemokines
T-cell Mediated Immunity
MHCII
MHCI
Immunity & defense
780938
Cd9
Ifitm3
Pglyrp1
ENSMUSG00000028268
Mpa2l
Aif1
ENSMUSG00000076722
ENSMUSG00000076703
Igh
Cd47
Gzma
Ccl6
Cd274
Ifit1
Igl-C1
Cxcr3
ENSMUSG00000072806
Ccl8
Cxcl10
Oasl2
Cxcl9
Fcgr3
Cxcr6
Ccl2
Lyz1
Igh-4
Fcgr4
Fyn
Fcer1g
ENSMUSG00000060586
ENSMUSG00000036322
Ccl5
Ifi203
Csf2ra
Tyrobp
Cd48
Tapbpl
Rrncs2
ENSMUSG00000076664
Zap70
Gbp1
H2-DMa
Cd99l2
Lsp1
Gzmb
Gbp2
H2-DMb1
EP3-1VL
Igh-1a
Irf1
Tcra
Saa2
ENSMUSG00000076549
C1qa
C1r
Lck
B2m
H2-L
Cd74
Ciita
Alox5ap
C1qc
Ptpn22
Ctsw
Cd1d1
Tap1
Clec4a3
Lyz2
Cd3d
H2-T9
Nkg7
Parp3
C1qb
Tap2
Cd3g
Clec2h
H2-T23
Samhd1
Gbp6
ENSMUSG00000076720
Clec4a1
ENSMUSG00000055413
Gimap4
Selplg
ENSMUSG00000076636
ENSMUSG00000076687
ENSMUSG00000076706
Gm1418
ENSMUSG00000076696
Textmining
Neighborhood
Cooccurrence
Gene Fusion
Coexpression
Experiments
Databases
[Homology]

Supplemental Figures

The microbiota mediates pathogen clearance from the gut lumen after non-typhoidal *Salmonella* diarrhea

Kathrin Endt*[1], Bärbel Stecher*[1], Samuel Chaffron[2], Emma Slack[3], Nicolas Tchitchek[4], Arndt Benecke[4], Laurye Van Maele[5], Jean-Claude Sirard[5], Andreas J. Mueller[1], Mathias Heikenwalder[6], Andrew J. Macpherson[3], Richard Strugnell[7], Christian von Mering[2] and Wolf-Dietrich Hardt[1#]

Table S1. Bacterial strains and Plasmids used in this study

Strain	Genotype and antibiotic resistance	Phenotype	Source or reference
S. tm ^{wt}	*S. tm* strain SL1344; strep^{R}	*S.typhimurium* wild type	[1]
S. tm^{att} (M556)	SL1344 *sseD*::*aphT;* strep^{R}, km^{R}	Induces gut inflammation via the SPI-1 TTSS; Lacks SPI-2 TTSS; attenuated in systemic infection	[2]
S. tm $^{\Delta O}$	SL1344Δ*wbaP;* strep^{R}	No O-antigen	[3]
S. tm^{avir} (M557)	SL1344 Δ*invG* *sseD::aphT,* strep^{R}, km^{R}	Lacks functional SPI-1 and SPI-2 TTSS; does not induce gut inflammation and is attenuated in systemic infection	[2]
M933	SL1344 Δ*invG*; *sseD*::*aphT*; *fliGHI*::Tn*10*; strep^{R}, km^{R}, tet^{R}	Lacks functional SPI-1, SPI-2 TTSS and flagella biosynthesis (no flagellin produced)	[4]
S.en wt	*S.en* strain 125109; strep^{R}	*S.enteritidis* wild type	[5]
S.en^{att} (M1512)	*S.en* 125109 Δ*ssaV::cat;* strep^{R}, cm^{R}	Induces gut inflammation via the SPI-1 TTSS; Lacks SPI-2 TTSS; attenuated in systemic infection	[5]
S.en^{avir} (M1513)	*S.en* 125109 *invC*::aphT; *ssaV::cat;* strep^{R}, km^{R}, cm^{R}	Lacks functional SPI-1 and SPI-2 TTSS; does not induce gut inflammation and is attenuated in systemic infection	[5]
Escherichia coli	*Nissle 1917 strain; wild type*		Kind gift of Dr. Sören

			Schubert
Lactobacillus reuteri	*Wild type*	Mouse gut isolate	[6]
Enterococcus faecalis	*Wild type*	Mouse gut isolate	This study
Plasmid	**Genotype and antibiotic resistance**	**Phenotype**	**Source or reference**
pM979	P_{rpsM} *gfpmut2 ori*pBR322; amp^R	Constitutive *gfp* expression	[7]
pM973	P_{ssaG} *gfpmut2 ori*pMB1 amp^R	Intracellular *gfp* expression; Indicator for Salmonella invaded into the gut mucosa; Used for 'challenge infections'	[8]
pWKS30	amp^R; *ori*pMB1		[9]

Table S2. Mice used in this study

Name	genetic background	microbiota*	colonization resistance	source or reference
Wild type mice (C)	C57BL/6	specific pathogen free (C)	yes	Rodent center HCI (RCHCI)
TCR $\beta^{-/-}\delta^{-/-}$	C57BL/6	specific pathogen free (C)	yes	[10]
JHT	C57BL/6	specific pathogen free (C)	yes	[11]
$IgA^{-/-}$	C57BL/6	specific pathogen free (C)	yes	[12]
$pIgR^{-/-}$	C57BL/6	specific pathogen free (C)	yes	[13]
L (LCM)	C57BL/6	low complexity microbiota	no	[14]

*C= conventional, specified pathogen free microbiota.

Table S3. Pathways significantly over-represented among the differentially expressed genes in the cecal mucosa of L-mice at day 40 p.i. with *S. tm* ^{att}

B-cell- and antibody-mediated immunity

PROBE	LOG_Q[090514_J-K_ind.ma2]	VAR[090514_J-K_ind.ma2]	P[090514_J-K_ind.ma2]	Celera Gene ID	Gene_Symbol	Gene_Name
429239	5.93180	0.93180	0.00000	mCG56372.2	LOC432699	null
339582	4.26380	0.89670	0.00000	mCG140410	Igh-1a|LOC544908	immunoglobulin heavy chain 1a (serum IgG2a)
590082	4.13340	0.85190	0.00000	mCG141789.1	Igk-V32	immunoglobulin kappa chain variable 32 (V32)
808065	3.99290	1.80190	0.00000	mCG130744.2|mCG1036427.2	LOC635601|bd2|LOC628027	null
736226	3.97930	1.02240	0.00000	mCG1027522.1|mCG1029835.1	LOC636462	null
401576	3.90870	1.76620	0.00000	mCG132002.2	LOC243439	null
891891	3.85240	1.34100	0.00000	mCG113660.1	LOC633515	null
538665	3.83340	0.58660	0.00000	null	LOC434031|Igk-V38	immunoglobulin kappa chain variable 38(V38)
491036	3.77740	0.84550	0.00000	mCG116913.1	LOC636067	null
699266	3.77400	0.76790	0.00000	mCG1025451.1	null	null
742698	3.74840	0.88410	0.00000	mCG130744.2|mCG1036427.2|mCG1036498.2	LOC635664|LOC635601|bd2|LOC628056|LOC628027	null
493584	3.71590	0.98470	0.00000	mCG142153.1	LOC620105|LOC637047	null
411187	3.70140	0.56530	0.00000	null	LOC620017	null
348117	3.67230	0.45770	0.00000	mCG1036432.2	null	null
857940	3.65340	1.28650	0.00000	mCG1037662.1	LOC630251	null
715331	3.64830	0.51560	0.00000	mCG141621.1	LOC434037	null
901486	3.64130	1.45140	0.00000	mCG68149.2	LOC630331|LOC633472	null
596021	3.63320	1.11870	0.00000	mCG146921.1|mCG141794.1|mCG141802.1	IgM	null
574582	3.58730	1.10810	0.00000	mCG146921.1|mCG141794.1	IgM	null
515370	3.58010	1.03810	0.00000	mCG142162.1	LOC626145|LOC545854	null
444829	3.55200	1.23660	0.00000	mCG141790.1	Gm1067	gene model 1067, (NCBI)
489583	3.43750	0.72290	0.00000	mCG114300.1	null	null
479671	3.42090	0.74830	0.00000	mCG126269.2|mCG1036505.2	gn33|Igk-V34|Igk-V33	immunoglobulin kappa chain variable 34 (V34)|immunoglobulin kappa chain variable 33 (V33)
896758	3.41680	0.08000	0.00000	mCG1037964.1	LOC620216|LOC632220	null
583890	3.36590	0.47530	0.00000	mCG117763.1	LOC634652|LOC382695|LOC436124	null
919480	3.30590	0.97960	0.00000	mCG141784.1	LOC434025	null
675426	3.26900	0.99890	0.00000	mCG128543.1	Igh-1a|LOC382692|LOC628614	immunoglobulin heavy chain 1a (serum IgG2a)
823783	3.23050	0.56160	0.00000	mCG1036439.2	LOC384413|Igk-V28	immunoglobulin kappa chain variable 28 (V28)
899105	3.22980	0.41100	0.00000	mCG142070	LOC637785	null
739642	3.18500	0.52560	0.00000	mCG141793.1	LOC434026	null
898268	3.16270	0.52810	0.00000	mCG127559.1|mCG114359	LOC640614|LOC632997|LOC636453	null
317586	3.15470	0.98640	0.00010	mCG1025125.1	LOC631518	null
576556	3.14730	1.11630	0.00000	mCG140401	LOC634430	null
902557	3.11220	0.71020	0.00000	mCG127559.1	null	null
843602	3.08470	0.78140	0.00000	mCG118954	LOC638634	null
897561	3.08440	0.54880	0.00000	null	LOC434609	null
483305	3.08070	0.65440	0.00000	null	Gm1419	gene model 1419, (NCBI)
901720	3.07910	0.51480	0.00000	mCG1026782.1	LOC382695|LOC629938|LOC638485	null
523804	3.01550	0.22180	0.00000	mCG1037963.1	LOC632180|LOC432993|LOC620169	null
875823	2.97880	0.64400	0.00000	mCG129378	LOC544903	null
410888	2.95830	0.97940	0.00000	mCG1025140.1	LOC633734	null
672387	2.94750	1.17050	0.00000	mCG114360|mCG1025864.1	null	null
401803	2.93560	0.50790	0.00000	mCG118868.1	LOC634298	null
615665	2.92850	0.88010	0.00000	mCG1050179	D6Mit97|Igk-V28	DNA segment, Chr 6, Massachusetts Institute of Technology 97|immunoglobulin kappa chain variable 28 (V28)
579252	2.92670	0.63600	0.00000	mCG127631.1	Igh-4	immunoglobulin heavy chain 4 (serum IgG1)
832392	2.90250	0.86180	0.00000	null	LOC628127	null
894906	2.89830	0.71310	0.00000	mCG118865.1|mCG114299.1	LOC629884|LOC637000|Igh|Igh-VJ558	immunoglobulin heavy chain complex|immunoglobulin heavy chain (J558 family)
899101	2.79970	1.08000	0.00000	mCG129262.1	Igh-VJ558	immunoglobulin heavy chain (J558 family)
893766	2.79370	0.47810	0.00000	mCG116911.1|mCG142745|mCG142069	LOC619833|LOC382696|LOC637398|LOC637794|VH18	immunoglobulin heavy chain (J558 family)
894845	2.79170	0.66090	0.00000	mCG1036509.2|mCG141633.1|mCG141637.1	LOC628516|LOC636646|LOC636598|LOC628498	null
621943	2.75070	0.43730	0.00000	mCG127630.1	LOC633062	null
797351	2.73710	0.26570	0.00000	mCG118871.1|mCG114299.1|mCG140407	Igh-1a|LOC634338|LOC629884|LOC629871|LOC63422	immunoglobulin heavy chain 1a (serum IgG2a)|immunoglobulin heavy chain complex|immunoglobulin heavy chain (J558 family)
721976	2.72350	0.78620	0.00000	mCG141796.1	LOC545847	null
892758	2.68780	0.73590	0.00000	mCG118870.1	LOC634541	null
685068	2.68190	0.96900	0.00000	mCG131876.2	null	null
902558	2.67750	0.53460	0.00000	mCG124907.1	null	null
374491	2.67550	0.61830	0.00000	mCG1036507.2	null	null
902338	2.66330	0.51890	0.00000	mCG129972.1	LOC638099|LOC629893	null
400498	2.62390	0.75150	0.00000	mCG141610.1	null	null
892044	2.60960	0.42700	0.00000	mCG1025954.1	null	null
902277	2.60290	0.68610	0.00000	mCG113668	LOC633719	null
856087	2.58540	0.67150	0.00000	mCG1036442.2	null	null
566733	2.57470	0.93750	0.00000	mCG1026777	LOC639369	null
478281	2.56490	0.98540	0.00010	null	LOC243431	null
657549	2.55990	0.50810	0.00000	mCG1036441.2	LOC620357|LOC637227	null
896839	2.54630	0.47530	0.00000	mCG118864.1	LOC634081|LOC634275	null
497944	2.52610	1.03850	0.00000	null	LOC238418	null
395082	2.49490	0.24860	0.00000	mCG13668.2	LOC238447|LOC544903|LOC544907|Igh-VJ558	immunoglobulin heavy chain (J558 family)
411078	2.49050	0.82620	0.00000	mCG1036502.2|mCG132001.2	LOC434025|LOC243433|LOC628159|LOC635885	null
903525	2.42830	0.89490	0.00000	mCG1036509.2	LOC628516|LOC636646	null
892300	2.42540	1.12620	0.00000	mCG1032189.1	LOC629883	null
650375	2.40130	0.90540	0.00000	mCG142578	LOC213570|LOC636126	null
379964	2.39580	0.52100	0.00000	mCG1025534.1	LOC631129	null
658871	2.37950	0.82770	0.00000	mCG1036438.2|mCG141622.1	Gm1530|Gm1420	gene model 1530, (NCBI)|gene model 1420, (NCBI)
788195	2.35930	0.54530	0.00000	mCG141636.1	LOC545848	null
904211	2.35030	1.20470	0.00000	mCG142561	LOC629906|LOC629908|LOC634791	null
904213	2.34960	0.92070	0.00000	mCG118867	LOC634123	null
316223	2.32080	0.25740	0.00000	mCG1036431.2	ci12	null
658873	2.32030	0.95390	0.00000	mCG126268.2|mCG1036508.2|mCG141637.1|mCG1(	Gm1419|Igk-C|Gm459|LOC546244|LOC619635	gene model 1419, (NCBI)|immunoglobulin kappa chain, constant region|gene model 459, (NCBI)
380936	2.28220	0.78480	0.00000	mCG1036436.1	Gm1418	gene model 1418, (NCBI)
823261	2.28190	0.88690	0.00000	mCG126265.2|mCG141634.1	Gm1419|Gm1524|LOC546244	gene model 1419, (NCBI)|gene model 1524, (NCBI)
900977	2.26030	0.91220	0.00000	mCG141630.1	LOC434586	null
894197	2.24640	0.93230	0.00000	mCG116912.1	null	null
557237	2.21780	0.33990	0.00000	mCG146830	LOC634450|LOC625794|LOC624610	null
904212	2.19090	0.91540	0.00000	mCG118865.1	LOC629906|LOC634065|LOC245266	null
372826	2.08430	0.75830	0.00000	mCG141629.1	null	null
910033	1.85080	0.21260	0.00000	mCG131871.2	Igk-V8|LOC545854|Igk-C|LOC243469|Igk-V21|Igk-V28	immunoglobulin kappa chain variable 8 (V8)|immunoglobulin kappa chain, constant region|immunoglobulin kappa chain variable 21 (V21)|immunoglobulin kappa chain variable 2
388152	1.84420	0.96390	0.00000	null	LOC628571	null
305669	1.83780	0.57610	0.00000	mCG142176.1	Igk-V8|LOC637207	immunoglobulin kappa chain variable 8 (V8)

456277	1.78790	0.37940	0.00000	mCG8631.2	Fcgr3a	Fc fragment of IgG, low affinity IIIa, receptor
409578	1.76210	0.53860	0.00000	mCG142168.1|mCG142181.1	LOC620191|LOC637126	null
815506	1.75880	0.68830	0.00020	mCG142169.1	LOC637295|LOC620451	null
895899	1.75600	0.75600	0.00050	mCG127250	LOC638631	null
902343	1.60140	0.51470	0.00000	mCG116911.1	LOC619833|LOC635935|Igh-VJ558	immunoglobulin heavy chain (J558 family)
897263	1.48890	0.24630	0.00000	mCG142552	null	null
910246	1.44630	0.59210	0.00000	mCG142161.1|mCG1036517.2	Igk-V21	immunoglobulin kappa chain variable 21 (V21)
912624	1.37490	0.62600	0.00000	mCG141777	LOC433053|LOC623736|Igl-V1	immunoglobulin lambda chain, variable 1
909884	1.36870	0.41510	0.00000	mCG141776|mCG141779	Igl-V1|2010309G21Rik	immunoglobulin lambda chain, variable 1|RIKEN cDNA 2010309G21 gene
649745	0.92060	0.38690	0.00100	mCG8629.2	Fcgr3	Fc receptor, IgG, low affinity III
774411	0.86170	0.23540	0.00000	mCG144561	Alox5ap	arachidonate 5-lipoxygenase activating protein
465504	0.81420	0.31440	0.00020	mCG8632.2	Fcer1g	Fc receptor, IgE, high affinity I, gamma polypeptide
323019	0.65580	0.08400	0.00000	mCG132542.2	Clec2h	C-type lectin domain family 2, member h

Cytokine and chemokine mediated signaling pathway

PROBE	LOG_Q[090514_J-K_ind.ma2]	VAR[090514_J-K_ind.ma2]	P[090514_J-K_ind.ma2]	Celera Gene ID	Gene_Symbol	Gene_Name
575878	4.39140	0.41670	0.00000	mCG12528.2	Cxcl9	chemokine (C-X-C motif) ligand 9
930152	3.26280	0.49470	0.00000	mCG12531.2	Cxcl10	chemokine (C-X-C motif) ligand 10
624929	2.74780	0.48220	0.00000	mCG2202.1	Cxcr3	chemokine (C-X-C motif) receptor 3
801088	2.46720	0.63340	0.00000	mCG15845.2	Cxcr6	chemokine (C-X-C motif) receptor 6
516139	2.40280	0.34790	0.00000	mCG11684.1	Ccl5	chemokine (C-C motif) ligand 5
907844	1.54020	0.56760	0.00000	mCG8184.2	Ccl2	chemokine (C-C motif) ligand 2
928327	1.26980	0.21370	0.00000	mCG11623.1	Ccl6	chemokine (C-C motif) ligand 6
753313	1.10330	0.55180	0.00000	mCG123600|mCG114938	Ccl8	chemokine (C-C motif) ligand 8
665530	0.55120	0.08910	0.00060	mCG20697.2	Csf2ra	colony stimulating factor 2 receptor, alpha, low-affinity (granulocyte-macrophage)

Cytokine/chemokine mediated immunity

PROBE	LOG_Q[090514_J-K_ind.ma2]	VAR[090514_J-K_ind.ma2]	P[090514_J-K_ind.ma2]	Celera Gene ID	Gene_Symbol	Gene_Name
575878	4.39140	0.41670	0.00000	mCG12528.2	Cxcl9	chemokine (C-X-C motif) ligand 9
930152	3.26280	0.49470	0.00000	mCG12531.2	Cxcl10	chemokine (C-X-C motif) ligand 10
624929	2.74780	0.48220	0.00000	mCG2202.1	Cxcr3	chemokine (C-X-C motif) receptor 3
801088	2.46720	0.63340	0.00000	mCG15845.2	Cxcr6	chemokine (C-X-C motif) receptor 6
516139	2.40280	0.34790	0.00000	mCG11684.1	Ccl5	chemokine (C-C motif) ligand 5
907844	1.54020	0.56760	0.00000	mCG8184.2	Ccl2	chemokine (C-C motif) ligand 2
928327	1.26980	0.21370	0.00000	mCG11623.1	Ccl6	chemokine (C-C motif) ligand 6
753313	1.10330	0.55180	0.00000	mCG123600|mCG114938	Ccl8	chemokine (C-C motif) ligand 8

Immunity and defense

PROBE	LOG_Q[090514_J-K_ind.ma2]	VAR[090514_J-K_ind.ma2]	P[090514_J-K_ind.ma2]	Celera Gene ID	Gene_Symbol	Gene_Name
429239	5.93180	0.93180	0.00000	mCG56372.2	LOC432699	null
550292	5.23590	1.24620	0.00000	mCG4516.2	Gzma	granzyme A
575878	4.39140	0.41670	0.00000	mCG12528.2	Cxcl9	chemokine (C-X-C motif) ligand 9
339582	4.26380	0.89670	0.00000	mCG140410	Igh-1a|LOC544908	immunoglobulin heavy chain 1a (serum IgG2a)
590082	4.13340	0.85190	0.00000	mCG141789.1	Igk-V32	immunoglobulin kappa chain variable 32 (V32)
808065	3.99290	1.80190	0.00000	mCG130744.2|mCG1036427.2	LOC635601|bd2|LOC628027	null
736226	3.97930	1.02240	0.00000	mCG1027522.1|mCG1029835.1	LOC636462	null
401576	3.90870	1.76620	0.00000	mCG132002.2	LOC243439	null
891891	3.85240	1.34100	0.00000	mCG113660.1	LOC633515	null
538665	3.83340	0.58660	0.00000	null	LOC434031|Igk-V38	immunoglobulin kappa chain variable 38(V38)
491036	3.77740	0.84550	0.00000	mCG116913.1	LOC636067	null
699266	3.77400	0.76790	0.00000	mCG1025451.1	null	null
742698	3.74840	0.88410	0.00000	mCG130744.2|mCG1036427.2|mCG1036498.2	LOC635664|LOC635601|bd2|LOC628056|LOC628027	null
493584	3.71590	0.98470	0.00000	mCG142153.1	LOC620105|LOC637047	null
411187	3.70140	0.56530	0.00000	null	LOC620017	null
348117	3.67230	0.45770	0.00000	mCG1036432.2	null	null
857940	3.65340	1.28650	0.00000	mCG1037662.1	LOC630251	null
715331	3.64830	0.51560	0.00000	mCG141621.1	LOC434037	null
901486	3.64130	1.45140	0.00000	mCG68149.2	LOC630331|LOC633472	null
596021	3.63320	1.11870	0.00000	mCG146921.1|mCG141794.1|mCG141802.1	IgM	null
574582	3.58730	1.10810	0.00000	mCG146921.1|mCG141794.1	IgM	null
515370	3.58010	1.03810	0.00000	mCG142162.1	LOC626145|LOC545854	null
444829	3.55200	1.23660	0.00000	mCG141790.1	Gm1067	gene model 1067, (NCBI)
489583	3.43750	0.72290	0.00000	mCG114300.1	null	null
479671	3.42090	0.74830	0.00000	mCG126269.2|mCG1036505.2	gn33|Igk-V34|Igk-V33	immunoglobulin kappa chain variable 34 (V34)|immunoglobulin kappa chain variable 33 (V33)
896758	3.41680	0.08000	0.00000	mCG1037964.1	LOC620216|LOC632220	null
583890	3.36590	0.47530	0.00000	mCG117763.1	LOC634652|LOC382695|LOC436124	null
919480	3.30590	0.97960	0.00000	mCG141784.1	LOC434025	null
675426	3.26900	0.99890	0.00000	mCG128543.1	Igh-1a|LOC382692|LOC628614	immunoglobulin heavy chain 1a (serum IgG2a)
930152	3.26280	0.49470	0.00000	mCG12531.2	Cxcl10	chemokine (C-X-C motif) ligand 10
823783	3.23050	0.56160	0.00000	mCG1036439.2	LOC384413|Igk-V28	immunoglobulin kappa chain variable 28 (V28)
899105	3.22980	0.41100	0.00000	mCG142070	LOC637785	null
739642	3.18500	0.52560	0.00000	mCG141793.1	LOC434026	null
898268	3.16270	0.52810	0.00000	mCG127559.1|mCG114359	LOC640614|LOC632997|LOC636453	null
317586	3.15470	0.98640	0.00010	mCG1025125.1	LOC631518	null
576556	3.14730	1.11630	0.00000	mCG140401	LOC634430	null
902557	3.11220	0.71020	0.00000	mCG127559.1	null	null
843602	3.08470	0.78140	0.00000	mCG118954	LOC638634	null
897561	3.08440	0.54880	0.00000	null	LOC434609	null
483305	3.08070	0.65440	0.00000	null	Gm1419	gene model 1419, (NCBI)
901720	3.07910	0.51480	0.00000	mCG1026782.1	LOC382695|LOC629938|LOC638485	null
523804	3.01550	0.22180	0.00000	mCG1037963.1	LOC632180|LOC432993|LOC620169	null
875823	2.97880	0.64400	0.00000	mCG129378	LOC544903	null
410888	2.95830	0.97940	0.00000	mCG1025140.1	LOC633734	null
672387	2.94750	1.17050	0.00000	mCG114360|mCG1025864.1	null	null
401803	2.93560	0.50790	0.00000	mCG118868.1	LOC634298	null
615665	2.92850	0.88010	0.00000	mCG1050179	D6Mit97|Igk-V28	DNA segment, Chr 6, Massachusetts Institute of Technology 97|immunoglobulin kappa chain variable 28 (V28)
579252	2.92670	0.63600	0.00000	mCG127631.1	Igh-4	immunoglobulin heavy chain 4 (serum IgG1)
832392	2.90250	0.86180	0.00000	null	LOC628127	null
894906	2.89830	0.71310	0.00000	mCG118865.1|mCG114299.1	LOC629884|LOC637000|Igh|Igh-VJ558	immunoglobulin heavy chain complex|immunoglobulin heavy chain (J558 family)
884118	2.80080	1.03780	0.00040	mCG130827	Gzmb	granzyme B

899101	2.79970	1.08000	0.00000	mCG129262.1	Igh-VJ558	immunoglobulin heavy chain (J558 family)
893766	2.79370	0.47810	0.00000	mCG116911.1|mCG142745|mCG142069	LOC619833|LOC382696|LOC637398|LOC637794|VH18	immunoglobulin heavy chain (J558 family)
894845	2.79170	0.66090	0.00000	mCG1036509.2|mCG141633.1|mCG141637.1	LOC628516|LOC636646|LOC636598|LOC628498	null
621943	2.75070	0.43730	0.00000	mCG127630.1	LOC633062	null
624929	2.74780	0.48220	0.00000	mCG2202.1	Cxcr3	chemokine (C-X-C motif) receptor 3
797351	2.73710	0.26570	0.00000	mCG118871.1|mCG114299.1|mCG140407	Igh-1a|LOC634338|LOC629884|LOC629871|LOC63422	immunoglobulin heavy chain 1a (serum IgG2a)|immunoglobulin heavy chain complex|immunoglobulin heavy chain (J558 family)
721976	2.72350	0.78620	0.00000	mCG141796.1	LOC545847	null
892758	2.68780	0.73590	0.00000	mCG118870.1	LOC634541	null
685068	2.68190	0.96900	0.00000	mCG131876.2	null	null
902558	2.67750	0.53460	0.00000	mCG124907.1	null	null
374491	2.67550	0.61830	0.00000	mCG1036507.2	null	null
902338	2.66330	0.51890	0.00000	mCG129972.1	LOC638099|LOC629893	null
712519	2.65430	0.25200	0.00000	null	H2-Q8	histocompatibility 2, Q region locus 8
400498	2.62390	0.75150	0.00000	mCG141610.1	null	null
586296	2.61800	0.56980	0.00010	mCG146987	Gbp1	guanylate nucleotide binding protein 1
892044	2.60960	0.42700	0.00000	mCG1025954.1	null	null
902277	2.60290	0.68610	0.00000	mCG113668	LOC633719	null
320903	2.58600	0.32230	0.00000	null	H2-Q1	histocompatibility 2, Q region locus 1
856087	2.58540	0.67150	0.00000	mCG1036442.2	null	null
566733	2.57470	0.93750	0.00000	mCG1026777	LOC639369	null
478281	2.56490	0.98540	0.00010	null	LOC243431	null
431279	2.56150	0.38030	0.00000	mCG113208.1	H2-Ea|H2-Aa	histocompatibility 2, class II antigen E alpha|histocompatibility 2, class II antigen A, alpha
657549	2.55990	0.50810	0.00000	mCG1036441.2	LOC620357|LOC637227	null
896839	2.54630	0.47530	0.00000	mCG118864.1	LOC634081|LOC634275	null
745275	2.54470	0.18670	0.00000	mCG23016.2	H2-DMa	histocompatibility 2, class II, locus DMa
497944	2.52610	1.03850	0.00000	null	LOC238418	null
395082	2.49490	0.24860	0.00000	mCG13668.2	LOC238447|LOC544903|LOC544907|Igh-VJ558	immunoglobulin heavy chain (J558 family)
411078	2.49050	0.82620	0.00000	mCG1036502.2|mCG132001.2	LOC434025|LOC243433|LOC628159|LOC635885	null
801088	2.46720	0.63340	0.00000	mCG15845.2	Cxcr6	chemokine (C-X-C motif) receptor 6
903525	2.42830	0.89490	0.00000	mCG1036509.2	LOC628516|LOC636646	null
892300	2.42540	1.12620	0.00000	mCG1032189.1	LOC629883	null
516139	2.40280	0.34790	0.00000	mCG11684.1	Ccl5	chemokine (C-C motif) ligand 5
650375	2.40130	0.90540	0.00000	mCG142578	LOC213570|LOC636126	null
379964	2.39580	0.52100	0.00000	mCG1025534.1	LOC631129	null
658871	2.37950	0.82770	0.00000	mCG1036438.2|mCG141622.1	Gm1530|Gm1420	gene model 1530, (NCBI)|gene model 1420, (NCBI)
847876	2.37220	0.26840	0.00000	mCG122229	Gbp2	guanylate nucleotide binding protein 2
788195	2.35930	0.54530	0.00000	mCG141636.1	LOC545848	null
904211	2.35030	1.20470	0.00000	mCG142561	LOC629906|LOC629908|LOC634791	null
904213	2.34960	0.92070	0.00000	mCG118867	LOC634123	null
316223	2.32080	0.25740	0.00000	mCG1036431.2	ci12	null
658873	2.32030	0.95390	0.00000	mCG126268.2|mCG1036508.2|mCG141637.1|mCG1(	Gm1419|Igk-C|Gm459|LOC546244|LOC619635	gene model 1419, (NCBI)|immunoglobulin kappa chain, constant region|gene model 459, (NCBI)
380936	2.28220	0.78480	0.00000	mCG1036436.1	Gm1418	gene model 1418, (NCBI)
823261	2.28190	0.88690	0.00000	mCG126265.2|mCG141634.1	Gm1419|Gm1524|LOC546244	gene model 1419, (NCBI)|gene model 1524, (NCBI)
637912	2.27350	0.18870	0.00000	mCG132704.1	H2-Ab1|LOC641240	histocompatibility 2, class II antigen A, beta 1
900977	2.26030	0.91220	0.00000	mCG141630.1	LOC434586	null
904963	2.25850	0.40890	0.00000	mCG132703.2|mCG132689.1	H2-DMb2|H2-DMb1	histocompatibility 2, class II, locus Mb2|histocompatibility 2, class II, locus Mb1
775978	2.24760	0.20400	0.00000	mCG6027.2	Cd74	CD74 antigen (invariant polypeptide of major histocompatibility complex, class II antigen-associated)
894197	2.24640	0.93230	0.00000	mCG116912.1	null	null
920968	2.22910	0.24630	0.00000	mCG9940.2	H2-Eb1	histocompatibility 2, class II antigen E beta
557237	2.21780	0.33990	0.00000	mCG146830	LOC634450|LOC625794|LOC624610	null
904212	2.19090	0.91540	0.00000	mCG118865.1	LOC629906|LOC634065|LOC245266	null
643417	2.17360	0.64740	0.00000	mCG124141	null	null
372826	2.08430	0.75830	0.00000	mCG141629.1	null	null
522474	2.05370	0.62000	0.00000	mCG126563.1	C2ta	class II transactivator
873670	2.02300	0.22280	0.00000	mCG23012.2	Tap1	transporter 1, ATP-binding cassette, sub-family B (MDR/TAP)
780747	1.99790	0.49670	0.00010	mCG127285.2	LOC636147|Cd8a	CD8 antigen, alpha chain
742215	1.96190	0.23130	0.00000	mCG8696.2	Tcra|LOC545051|A430107P09Rik	T-cell receptor alpha chain|RIKEN cDNA A430107P09 gene
447264	1.95530	0.48700	0.00030	mCG11758.2	Ctsw	cathepsin W
910033	1.85080	0.21260	0.00000	mCG131871.2	Igk-V8|LOC545854|Igk-C|LOC243469|Igk-V21|Igk-V28	immunoglobulin kappa chain variable 8 (V8)|immunoglobulin kappa chain, constant region|immunoglobulin kappa chain variable 21 (V21)|immunoglobulin kappa chain variable 2
388152	1.84420	0.96390	0.00000	null	LOC628571	null
305669	1.83780	0.57610	0.00000	mCG142176.1	Igk-V8|LOC637207	immunoglobulin kappa chain variable 8 (V8)
616423	1.80620	0.42350	0.00000	mCG20328.2	5830443L24Rik	RIKEN cDNA 5830443L24 gene
456277	1.78790	0.37940	0.00000	mCG8631.2	Fcgr3a	Fc fragment of IgG, low affinity IIIa, receptor
840423	1.78240	0.29170	0.00000	mCG1551.2	Cd3g	CD3 antigen, gamma polypeptide
405120	1.77250	0.22730	0.00000	mCG21119.2	Gbp4	guanylate nucleotide binding protein 4
409578	1.76210	0.53860	0.00000	mCG142168.1|mCG142181.1	LOC620191|LOC637126	null
815506	1.75880	0.68830	0.00020	mCG142169.1	LOC637295|LOC620451	null
895899	1.75600	0.75600	0.00050	mCG127250	LOC638631	null
453230	1.74770	0.32150	0.00000	mCG1536.1	Cd3d	CD3 antigen, delta polypeptide
913926	1.72950	0.51800	0.00000	mCG141961	9830147J24Rik	RIKEN cDNA 9830147J24 gene
613784	1.67590	0.37020	0.00000	mCG17747.2	Zap70	zeta-chain (TCR) associated protein kinase
902343	1.60140	0.51470	0.00000	mCG116911.1	LOC619833|LOC635935|Igh-VJ558	immunoglobulin heavy chain (J558 family)
501966	1.57600	0.44910	0.00000	mCG147911	B2m	beta-2 microglobulin
907844	1.54020	0.56760	0.00000	mCG8184.2	Ccl2	chemokine (C-C motif) ligand 2
897263	1.48890	0.24630	0.00000	mCG142552	null	null
910246	1.44630	0.59210	0.00000	mCG142161.1|mCG1036517.2	Igk-V21	immunoglobulin kappa chain variable 21 (V21)
917567	1.43150	0.27250	0.00000	mCG15923.1	Aif1	allograft inflammatory factor 1
912624	1.37490	0.62600	0.00000	mCG141777	LOC433053|LOC623736|Igl-V1	immunoglobulin lambda chain, variable 1
909884	1.36870	0.41510	0.00000	mCG141776|mCG141779	Igl-V1|2010309G21Rik	immunoglobulin lambda chain, variable 1|RIKEN cDNA 2010309G21 gene
909409	1.35240	0.42110	0.00000	mCG9333.2	C1qb	complement component 1, q subcomponent, beta polypeptide
607896	1.33990	0.28910	0.00000	mCG21470.1	Ifit1	interferon-induced protein with tetratricopeptide repeats 1
314727	1.32380	0.32000	0.00000	mCG10007.2	Cd48	CD48 antigen
351046	1.32030	0.18470	0.00000	mCG132214.1	Clec4a1	C-type lectin domain family 4, member a1
315737	1.30020	0.48310	0.00000	mCG3553.3	Selpl	selectin, platelet (p-selectin) ligand
928327	1.26980	0.21370	0.00000	mCG11623.1	Ccl6	chemokine (C-C motif) ligand 6
454874	1.23930	0.16550	0.00000	mCG6391.1	Ptpn22	protein tyrosine phosphatase, non-receptor type 22 (lymphoid)
736887	1.21900	0.11950	0.00000	mCG22139.1	Nkg7	natural killer cell group 7 sequence
737611	1.16720	0.29130	0.00000	null	Lck	lymphocyte protein tyrosine kinase
355529	1.15290	0.20110	0.00000	mCG132215.1	Clec4a3	C-type lectin domain family 4, member a3
753313	1.10330	0.55180	0.00000	mCG123600|mCG114938	Ccl8	chemokine (C-C motif) ligand 8
812906	1.08450	0.38480	0.00000	mCG144019	Saa2	serum amyloid A 2

440084	1.07700	0.18760	0.00000 mCG9108.1	Cd274	CD274 antigen
812669	1.06680	0.25910	0.00010 mCG3074.1	Cd1d1	CD1d1 antigen
604623	1.06550	0.09790	0.00000 null	Parp3	poly (ADP-ribose) polymerase family, member 3
524163	1.04600	0.18300	0.00000 mCG9327.1	C1qa	complement component 1, q subcomponent, alpha polypeptide
732899	1.04450	0.23180	0.00000 mCG141548	Oasl2	2'-5' oligoadenylate synthetase-like 2
374617	1.04100	0.22850	0.00000 mCG3049.3	Lyzs	lysozyme
897539	1.03280	0.07740	0.00000 mCG142248.1	LOC633551|C4|Slp	complement component 4 (within H-2S)|sex-limited protein
675339	1.02480	0.35290	0.00000 mCG9326.1	C1qg	complement component 1, q subcomponent, gamma polypeptide
925708	0.98980	0.20940	0.00000 mCG22590.1	Ifitm3	interferon induced transmembrane protein 3
922460	0.97840	0.09980	0.00000 mCG13768.1	Irf1	interferon regulatory factor 1
612867	0.97300	0.41510	0.00060 mCG128047.2	Gimap4	GTPase, IMAP family member 4
800022	0.96700	0.18650	0.00000 mCG22805.2	Tyrobp	TYRO protein tyrosine kinase binding protein
908953	0.94240	0.09150	0.00000 mCG11606.2	B2m	beta-2 microglobulin
649745	0.92060	0.38690	0.00100 mCG8629.2	Fcgr3	Fc receptor, IgG, low affinity III
923823	0.91860	0.24270	0.00000 mCG1253.1	Pglyrp1	peptidoglycan recognition protein 1
692814	0.90880	0.13390	0.00000 mCG21986.3	Samhd1	SAM domain and HD domain, 1
638437	0.88810	0.06670	0.00000 mCG132391.2	H2-T9|H2-T17|H2-T22|H2-T10	histocompatibility 2, T region locus 9|histocompatibility 2, T region locus 17|histocompatibility 2, T region locus 22|histocompatibility 2, T region locus 10
847591	0.87240	0.18830	0.00000 mCG134313.1	Tapbpl	TAP binding protein-like
774411	0.86170	0.23540	0.00000 mCG144561	Alox5ap	arachidonate 5-lipoxygenase activating protein
454213	0.85610	0.31890	0.00000 mCG3047.2	Lzp-s	P lysozyme structural
930739	0.84530	0.22190	0.00000 mCG141466	C1r	complement component 1, r subcomponent
465504	0.81420	0.31440	0.00020 mCG8632.2	Fcer1g	Fc receptor, IgE, high affinity I, gamma polypeptide
558496	0.79940	0.13770	0.00000 mCG12223.1	H2-T23	histocompatibility 2, T region locus 23
414909	0.78410	0.27060	0.00020 mCG6318.1	Ifi203	interferon activated gene 203
928306	0.77450	0.10840	0.00000 mCG23013.2	Tap2	transporter 2, ATP-binding cassette, sub-family B (MDR/TAP)
766362	0.74930	0.14560	0.00000 mCG125800.1	Fyn	Fyn proto-oncogene
334297	0.71020	0.20460	0.00010 null	Cd99	CD99 antigen
912733	0.67340	0.08560	0.00000 mCG129013.1	Cd47	CD47 antigen (Rh-related antigen, integrin-associated signal transducer)
323019	0.65580	0.08400	0.00000 mCG132542.2	Clec2h	C-type lectin domain family 2, member h
916013	0.64810	0.18630	0.00040 mCG11072.3	Lsp1	lymphocyte specific 1
675921	0.59630	0.06190	0.00000 mCG120898.1	LOC633897	null
351041	0.55290	0.08600	0.00040 mCG129426.1	Cd9	CD9 antigen
665530	0.55120	0.08910	0.00060 mCG20697.2	Csf2ra	colony stimulating factor 2 receptor, alpha, low-affinity (granulocyte-macrophage)

Interferon-mediated immunity

PROBE	LOG_Q[090514_J-K_ind.ma2]	VAR[090514_J-K_ind.ma2]	P[090514_J-K_ind.ma2]	Celera Gene ID	Gene_Symbol	Gene_Name
575878	4.39140	0.41670	0.00000	mCG12528.2	Cxcl9	chemokine (C-X-C motif) ligand 9
930152	3.26280	0.49470	0.00000	mCG12531.2	Cxcl10	chemokine (C-X-C motif) ligand 10
586296	2.61800	0.56980	0.00010	mCG146987	Gbp1	guanylate nucleotide binding protein 1
847876	2.37220	0.26840	0.00000	mCG122229	Gbp2	guanylate nucleotide binding protein 2
643417	2.17360	0.64740	0.00000	mCG124141	null	null
616423	1.80620	0.42350	0.00000	mCG20328.2	5830443L24Rik	RIKEN cDNA 5830443L24 gene
405120	1.77250	0.22730	0.00000	mCG21119.2	Gbp4	guanylate nucleotide binding protein 4
913926	1.72950	0.51800	0.00000	mCG141961	9830147J24Rik	RIKEN cDNA 9830147J24 gene
607896	1.33990	0.28910	0.00000	mCG21470.1	Ifit1	interferon-induced protein with tetratricopeptide repeats 1
732899	1.04450	0.23180	0.00000	mCG141548	Oasl2	2'-5' oligoadenylate synthetase-like 2
922460	0.97840	0.09980	0.00000	mCG13768.1	Irf1	interferon regulatory factor 1
414909	0.78410	0.27060	0.00020	mCG6318.1	Ifi203	interferon activated gene 203

MHCI-mediated immunity

PROBE	LOG_Q[090514_J-K_ind.ma2]	VAR[090514_J-K_ind.ma2]	P[090514_J-K_ind.ma2]	Celera Gene ID	Gene_Symbol	Gene_Name
712519	2.65430	0.25200	0.00000	null	H2-Q8	histocompatibility 2, Q region locus 8
320903	2.58600	0.32230	0.00000	null	H2-Q1	histocompatibility 2, Q region locus 1
780747	1.99790	0.49670	0.00010	mCG127285.2	LOC636147|Cd8a	CD8 antigen, alpha chain
447264	1.95530	0.48700	0.00030	mCG11758.2	Ctsw	cathepsin W
501966	1.57600	0.44910	0.00000	mCG147911	B2m	beta-2 microglobulin
908953	0.94240	0.09150	0.00000	mCG11606.2	B2m	beta-2 microglobulin
638437	0.88810	0.06670	0.00000	mCG132391.2	H2-T9|H2-T17|H2-T22|H2-T10	histocompatibility 2, T region locus 9|histocompatibility 2, T region locus 17|histocompatibility 2, T region locus 22|histocompatibility 2, T region locus 10
847591	0.87240	0.18830	0.00000	mCG134313.1	Tapbpl	TAP binding protein-like
558496	0.79940	0.13770	0.00000	mCG12223.1	H2-T23	histocompatibility 2, T region locus 23
675921	0.59630	0.06190	0.00000	mCG120898.1	LOC633897	null

MHCII-mediated immunity

PROBE	LOG_Q[090514_J-K_ind.ma2]	VAR[090514_J-K_ind.ma2]	P[090514_J-K_ind.ma2]	Celera Gene ID	Gene_Symbol	Gene_Name
431279	2.56150	0.38030	0.00000	mCG113208.1	H2-Ea|H2-Aa	histocompatibility 2, class II antigen E alpha|histocompatibility 2, class II antigen A, alpha
745275	2.54470	0.18670	0.00000	mCG23016.2	H2-DMa	histocompatibility 2, class II, locus DMa
637912	2.27350	0.18870	0.00000	mCG132704.1	H2-Ab1|LOC641240	histocompatibility 2, class II antigen A, beta 1
904963	2.25850	0.40890	0.00000	mCG132703.2|mCG132689.1	H2-DMb2|H2-DMb1	histocompatibility 2, class II, locus Mb2|histocompatibility 2, class II, locus Mb1
775978	2.24760	0.20400	0.00000	mCG6027.2	Cd74	CD74 antigen (invariant polypeptide of major histocompatibility complex, class II antigen-associated)
920968	2.22910	0.24630	0.00000	mCG9940.2	H2-Eb1	histocompatibility 2, class II antigen E beta
522474	2.05370	0.62000	0.00000	mCG126563.1	C2ta	class II transactivator

Macrophage-mediated immunity

PROBE	LOG_Q[090514_J-K_ind.ma2]	VAR[090514_J-K_ind.ma2]	P[090514_J-K_ind.ma2]	Celera Gene ID	Gene_Symbol	Gene_Name
575878	4.39140	0.41670	0.00000	mCG12528.2	Cxcl9	chemokine (C-X-C motif) ligand 9
930152	3.26280	0.49470	0.00000	mCG12531.2	Cxcl10	chemokine (C-X-C motif) ligand 10
586296	2.61800	0.56980	0.00010	mCG146987	Gbp1	guanylate nucleotide binding protein 1
847876	2.37220	0.26840	0.00000	mCG122229	Gbp2	guanylate nucleotide binding protein 2
616423	1.80620	0.42350	0.00000	mCG20328.2	5830443L24Rik	RIKEN cDNA 5830443L24 gene
456277	1.78790	0.37940	0.00000	mCG8631.2	Fcgr3a	Fc fragment of IgG, low affinity IIIa, receptor
405120	1.77250	0.22730	0.00000	mCG21119.2	Gbp4	guanylate nucleotide binding protein 4
913926	1.72950	0.51800	0.00000	mCG141961	9830147J24Rik	RIKEN cDNA 9830147J24 gene
351046	1.32030	0.18470	0.00000	mCG132214.1	Clec4a1	C-type lectin domain family 4, member a1
355529	1.15290	0.20110	0.00000	mCG132215.1	Clec4a3	C-type lectin domain family 4, member a3
649745	0.92060	0.38690	0.00100	mCG8629.2	Fcgr3	Fc receptor, IgG, low affinity III
774411	0.86170	0.23540	0.00000	mCG144561	Alox5ap	arachidonate 5-lipoxygenase activating protein

Natural killer cell mediated immunity

PROBE	LOG_Q[090514_J-K_ind.ma2]	VAR[090514_J-K_ind.ma2]	P[090514_J-K_ind.ma2]	Celera Gene ID	Gene_Symbol	Gene_Name
550292	5.23590	1.24620	0.00000	mCG4516.2	Gzma	granzyme A
447264	1.95530	0.48700	0.00030	mCG11758.2	Ctsw	cathepsin W

456277	1.78790	0.37940	0.00000	mCG8631.2	Fcgr3a	Fc fragment of IgG, low affinity IIIa, receptor
736887	1.21900	0.11950	0.00000	mCG22139.1	Nkg7	natural killer cell group 7 sequence
800022	0.96700	0.18650	0.00000	mCG22805.2	Tyrobp	TYRO protein tyrosine kinase binding protein
649745	0.92060	0.38690	0.00100	mCG8629.2	Fcgr3	Fc receptor, IgG, low affinity III
323019	0.65580	0.08400	0.00000	mCG132542.2	Clec2h	C-type lectin domain family 2, member h

T-cell mediated immunity

PROBE	LOG_Q[090514_J-K_ind.ma2]	VAR[090514_J-K_ind.ma2]	P[090514_J-K_ind.ma2]	Celera Gene ID	Gene_Symbol	Gene_Name
550292	5.23590	1.24620	0.00000	mCG4516.2	Gzma	granzyme A
712519	2.65430	0.25200	0.00000	null	H2-Q8	histocompatibility 2, Q region locus 8
320903	2.58600	0.32230	0.00000	null	H2-Q1	histocompatibility 2, Q region locus 1
431279	2.56150	0.38030	0.00000	mCG113208.1	H2-Ea|H2-Aa	histocompatibility 2, class II antigen E alpha|histocompatibility 2, class II antigen A, alpha
745275	2.54470	0.18670	0.00000	mCG23016.2	H2-DMa	histocompatibility 2, class II, locus DMa
637912	2.27350	0.18870	0.00000	mCG132704.1	H2-Ab1|LOC641240	histocompatibility 2, class II antigen A, beta 1
904963	2.25850	0.40890	0.00000	mCG132703.2|mCG132689.1	H2-DMb2|H2-DMb1	histocompatibility 2, class II, locus Mb2|histocompatibility 2, class II, locus Mb1
775978	2.24760	0.20400	0.00000	mCG6027.2	Cd74	CD74 antigen (invariant polypeptide of major histocompatibility complex, class II antigen-associated)
920968	2.22910	0.24630	0.00000	mCG9940.2	H2-Eb1	histocompatibility 2, class II antigen E beta
522474	2.05370	0.62000	0.00000	mCG126563.1	C2ta	class II transactivator
780747	1.99790	0.49670	0.00010	mCG127285.2	LOC636147|Cd8a	CD8 antigen, alpha chain
742215	1.96190	0.23130	0.00000	mCG8696.2	Tcra|LOC545051|A430107P09Rik	T-cell receptor alpha chain|RIKEN cDNA A430107P09 gene
447264	1.95530	0.48700	0.00030	mCG11758.2	Ctsw	cathepsin W
840423	1.78240	0.29170	0.00000	mCG1551.2	Cd3g	CD3 antigen, gamma polypeptide
453230	1.74770	0.32150	0.00000	mCG1536.1	Cd3d	CD3 antigen, delta polypeptide
501966	1.57600	0.44910	0.00000	mCG147911	B2m	beta-2 microglobulin
440084	1.07700	0.18760	0.00000	mCG9108.1	Cd274	CD274 antigen
812669	1.06680	0.25910	0.00010	mCG3074.1	Cd1d1	CD1d1 antigen
908953	0.94240	0.09150	0.00000	mCG11606.2	B2m	beta-2 microglobulin
638437	0.88810	0.06670	0.00000	mCG132391.2	H2-T9|H2-T17|H2-T22|H2-T10	histocompatibility 2, T region locus 9|histocompatibility 2, T region locus 17|histocompatibility 2, T region locus 22|histocompatibility 2, T region locus 10
847591	0.87240	0.18830	0.00000	mCG134313.1	Tapbpl	TAP binding protein-like
558496	0.79940	0.13770	0.00000	mCG12223.1	H2-T23	histocompatibility 2, T region locus 23
334297	0.71020	0.20460	0.00010	null	Cd99	CD99 antigen
675921	0.59630	0.06190	0.00000	mCG120898.1	LOC633897	null

Table S4. Quantitative Microbiota analysis by 454 amplicon sequencing

	Chao 1	Shannon (H)	E
S. tm ^{att} L (d.2)	49±15	0.4±0.4	0.1±0.1
S. tm ^{att} L (d.40)	62±14	0.8±0.3	0.2±0.1
S. tm ^{att} L (d.83)	53±31	0.4±0.3	0.1±0
S. tm ^{att} L /C	504±46	4.6±0.1	0.8±0
C	423	4.5	0.8

***** The **Shannon-index** (H') is a measure of species diversity taking into account the number of species and the evenness of the species. i =number of species: p_i= relative abundance of species i; H' is maximal if all species are present at equal abundance (H^{max} = log(1/i); i = number of species).

$$H' = -\sum_i p_i \cdot \ln p_i$$

 # Species Evenness: H'/H^{max}; (0-1) An E value of 1 means that the abundance of all species is the same.

‡ The **Chao1 estimato**r estimates total species richness as

$$SChao1 = Sobs + \frac{n1}{2n2}$$

where S_{obs} is the number of observed species, n_1 is the number of singletons (species captured once), and n_2 is the number of doubletons (species captured twice) [15].

Supplemental References

1. Hoiseth SK, Stocker BA (1981) Aromatic-dependent *Salmonella typhimurium* are non-virulent and effective as live vaccines. Nature 291: 238-239.

2. Hapfelmeier S, Ehrbar K, Stecher B, Barthel M, Kremer M, et al. (2004) Role of the Salmonella Pathogenicity Island 1 Effector Proteins SipA, SopB, SopE, and SopE2 in Salmonella enterica Subspecies 1 Serovar Typhimurium Colitis in Streptomycin-Pretreated Mice. Infect Immun 72: 795-809.

3. Ilg K, Endt K, Misselwitz B, Stecher B, Aebi M, et al. (2009) O-antigen-negative Salmonella enterica serovar Typhimurium is attenuated in intestinal colonization but elicits colitis in streptomycin-treated mice. Infect Immun 77: 2568-2575.

4. Stecher B, Barthel M, Schlumberger MC, Haberli L, Rabsch W, et al. (2008) Motility allows S. Typhimurium to benefit from the mucosal defence. Cell Microbiol 10: 1166-1180.

5. Suar M, Jantsch J, Hapfelmeier S, Kremer M, Stallmach T, et al. (2006) Virulence of broad- and narrow-host-range Salmonella enterica serovars in the streptomycin-pretreated mouse model. Infect Immun 74: 632-644.

6. Stecher B, Robbiani R, Walker AW, Westendorf AM, Barthel M, et al. (2007) Salmonella enterica Serovar Typhimurium Exploits Inflammation to Compete with the Intestinal Microbiota. PLoS Biol 5: e244.

7. Stecher B, Hapfelmeier S, Muller C, Kremer M, Stallmach T, et al. (2004) Flagella and Chemotaxis Are Required for Efficient Induction of Salmonella enterica Serovar Typhimurium Colitis in Streptomycin-Pretreated Mice. Infect Immun 72: 4138-4150.

8. Hapfelmeier S, Muller AJ, Stecher B, Kaiser P, Barthel M, et al. (2008) Microbe sampling by mucosal dendritic cells is a discrete, MyD88-independent step in DeltainvG S. Typhimurium colitis. J Exp Med 205: 437-450.

9. Wang RF, Kushner SR (1991) Construction of versatile low-copy-number vectors for cloning, sequencing and gene expression in Escherichia coli. Gene 100: 195-199.

10. Mombaerts P, Mizoguchi E, Ljunggren HG, Iacomini J, Ishikawa H, et al. (1994) Peripheral lymphoid development and function in TCR mutant mice. Int Immunol 6: 1061-1070.

11. Chen J, Trounstine M, Alt FW, Young F, Kurahara C, et al. (1993) Immunoglobulin gene rearrangement in B cell deficient mice generated by targeted deletion of the JH locus. Int Immunol 5: 647-656.

12. Harriman GR, Bogue M, Rogers P, Finegold M, Pacheco S, et al. (1999) Targeted deletion of the IgA constant region in mice leads to IgA deficiency with alterations in expression of other Ig isotypes. J Immunol 162: 2521-2529.

13. Johansen FE, Pekna M, Norderhaug IN, Haneberg B, Hietala MA, et al. (1999) Absence of epithelial immunoglobulin A transport, with increased mucosal leakiness, in polymeric immunoglobulin receptor/secretory component-deficient mice. J Exp Med 190: 915-922.

14. Stecher B, Chaffron S, Kappeli R, Hapfelmeier S, Freedrich S, et al. (2010) Like will to like: abundances of closely related species can predict susceptibility to intestinal colonization by pathogenic and commensal bacteria. PLoS Pathog 6: e1000711.

15. Hughes JB, Hellmann JJ, Ricketts TH, Bohannan BJ (2001) Counting the uncountable: statistical approaches to estimating microbial diversity. Appl Environ Microbiol 67: 4399-4406.